

# $D\bar{D}$ production and their interactions

Yan-Rui Liu\*

*Department of Physics, H-27, Tokyo Institute of Technology, Meguro, Tokyo 152-8551, Japan  
Institute of High Energy Physics, P.O. Box 918-4, Beijing 100049, People's Republic of China*

Makoto Oka†

*Department of Physics, H-27, Tokyo Institute of Technology, Meguro, Tokyo 152-8551, Japan*

Makoto Takizawa‡

*Showa Pharmaceutical University, Machida, Tokyo 194-8543, Japan*

Xiang Liu

*School of Physical Science and Technology, Lanzhou University, Lanzhou 730000, People's Republic of China*

Wei-Zhen Deng and Shi-Lin Zhu§

*Department of Physics, Peking University, Beijing 100871, People's Republic of China*

(Dated: February 10, 2018)

S- and P- wave  $D\bar{D}$  scatterings are studied in a meson exchange model with the coupling constants obtained in the heavy quark effective theory. With the extracted P- wave phase shifts and the separable potential approximation, we include the  $D\bar{D}$  rescattering effect and investigate the production process  $e^+e^- \rightarrow D\bar{D}$ . We find that it is difficult to explain the anomalous line shape observed by the BES Collaboration with this mechanism. Combining our model calculation and the experimental measurement, we estimate the upper limit of the nearly universal cutoff parameter to be around 2 GeV. With this number, the upper limits of the binding energies of the S- wave  $D\bar{D}$  and  $B\bar{B}$  bound states are obtained. Assuming that the S- wave and P- wave interactions rely on the same cutoff, our study provides a way of extracting the information about S- wave molecular bound states from the P- wave meson pair production.

PACS numbers: 12.39.Pn, 12.40.Yx, 13.75.Lb, 13.66.Bc

## I. INTRODUCTION

Recently observed charmoniumlike states, called  $X$ ,  $Y$  or  $Z$ , have motivated heated discussions on their properties (see Refs. [1–5] for the detailed review). All of them are above the  $D\bar{D}$  threshold and most states are near thresholds of two mesons. Various interpretations have been proposed, such as tetraquark or S-wave molecular states, hybrid states, dynamically generated states, or mixing states of  $c\bar{c}$  state and exotic components, while the possibility that they are just  $c\bar{c}$  states has not been excluded yet [6, 7]. Among these possibilities, the molecular interpretation is worth consideration, because the molecular states are expected to appear near the threshold.

To understand whether the proposed molecules exist or not, one may study the bound state solution of the heavy meson-antimeson systems. The meson exchange models are widely used in describing interactions of two hadrons [8–17]. Other approaches include the gluon exchange models [18, 19] the unitarized model [20], lattice QCD [21], and QCD sum rule formalism [22]. According to these theoretical calculations, it seems that the existence of heavy quark molecules is inevitable, especially for the isoscalar hidden bottom states, which awaits the future experimental confirmation.

Among the hidden-charm meson-meson systems, the  $D\bar{D}$  system is the simplest one. Since  $D$  is a pseudoscalar meson, the total angular momentum of the system is equal to the orbital momentum. The possible quantum numbers of the system are  $J^{PC} = 0^{++}, 1^{--}, 2^{++}$ , etc. There is no mixing between different partial waves, unlike in the case of the deuteron or  $D\bar{D}^*$ , where for instance the  $S - D$ - wave mixings are important. For the other charm meson and

---

\*Electronic address: yrliu@th.phys.titech.ac.jp

†Electronic address: oka@th.phys.titech.ac.jp

‡Electronic address: takizawa@ac.shoyaku.ac.jp

§Electronic address: zhustl@pku.edu.cn

anticharm meson system, there may exist open charm decay channels which renders the analysis more complicated. So we focus on the  $D\bar{D}$  system and discuss the isoscalar case within one meson exchange model intensively.

The investigations in the literatures indicate that such a scalar  $D\bar{D}$  bound/resonance state may exist. In fact, a  $D\bar{D}$  bound state was obtained around 3.1 MeV in a quark-based model [18]. A quasibound state was also found with the unitarized method [20, 23]. The vector meson exchange results in a possible binding solution [9]. Our previous results cannot exclude its existence within the meson exchange framework [14] and chiral quark model [16], either. However, a very recent analysis indicates that the existence of a  $D\bar{D}$  bound state is difficult to understand [24]. In this paper, we will reanalyze this issue.

Despite these efforts, the interaction in the heavy meson systems is still poorly known. It is expected that the study of the scattering provides us with additional information besides solving the bound state problems. For example, the S- wave  $DK$  scattering lengths and phase shifts give us additional information about whether the molecular interpretation for  $D_{sJ}(2317)$  is reasonable or not [25]. The scattering of  $D$  and  $D^*$  off the  $X(3872)$  may reflect the  $D\bar{D}^*$  interaction if  $X(3872)$  is a molecular state [26]. To better understand whether the  $D\bar{D}$  system may form a bound state, we will calculate the partial wave scattering phase shifts and the relevant cross sections. This is the first major part of the present study.

In addition to the observation of these unexpected hidden-charm X, Y, Z mesons, the BES Collaboration recently announced an anomalous line shape of the  $e^+e^- \rightarrow$  hadrons total cross sections in Ref. [27]. The structure is slightly above the  $D\bar{D}$  threshold and slightly lower than  $\psi(3770)$ . A similar anomalous line shape was also observed in the  $D\bar{D}$  production [28]. The di-resonance assumption is one possible choice to understand such a structure [29]. However, it is difficult to identify just from the cross section whether this structure is due to a bound state, a resonance or the final state interactions (FSI). More studies are required.

The dominant decay mode of  $\psi(3770)$  is the P- wave  $D\bar{D}$ . The FSI effects [30, 31] have been considered in understanding its large non- $D\bar{D}$  decay observed by BES [32, 33]. Their results indicate that FSI has non-negligible contributions. If the  $D\bar{D}$  interaction were really strong, the rescattering effect would also lead to the anomalous line shape in their production. In Ref. [34], part of the FSI effects in the  $D\bar{D}$  production has been included. No anomalous line shape appears. Here, we will study the rescattering effects in the process  $e^+e^- \rightarrow D\bar{D}$  based on the calculated phase shifts and the Yamaguchi separable potential approximation [35]. Therefore, the multiple scattering effects are included. This is the other major part of the present study.

With a heavier meson mass, a smaller kinetic energy and nearly the same potentials according to the heavy quark symmetry, the bottom analogous systems are more interesting. We will extend our study to the isoscalar  $B\bar{B}$  cases.

We organize our paper as follows. In Sec. II, we present the relevant Lagrangian, the derived potentials, and the definition of the threshold parameters. The numerical results for the S- and P- wave  $D\bar{D}$  systems are given in Secs. III and IV, respectively. In Sec. V, we consider the rescattering effect in  $e^+e^- \rightarrow D\bar{D}$ . In Sec. VI, the results for the  $B\bar{B}$  cases are presented. The last section is our discussion.

## II. THE EFFECTIVE POTENTIAL AND THRESHOLD PARAMETERS

One pion exchange between  $D$  and  $\bar{D}$  is forbidden because of the parity conservation. What we need are the couplings of the  $D$  meson with the light scalar and vector mesons. The relevant effective Lagrangian in the heavy quark limit reads [10, 36, 37]

$$\mathcal{L} = g_\sigma Tr[H\sigma\bar{H}] - i\beta_V Tr[Hv^\mu\rho_\mu\bar{H}], \quad (1)$$

where the field  $H$  denotes the degenerate  $(0^-, 1^-)$  doublet

$$H = \frac{1+\not{v}}{2}[P^{*\mu}\gamma_\mu + iP\gamma_5], \quad (2)$$

and  $v^\mu = (1, 0, 0, 0)$  denotes the velocity of the heavy mesons. The vector meson field has the form

$$\rho_\mu = i\frac{g_V}{\sqrt{2}}\hat{\rho}_\mu, \quad \hat{\rho}_\mu = \begin{pmatrix} \frac{\rho^0}{\sqrt{2}} + \frac{\omega}{\sqrt{2}} & \rho^+ & K^{*+} \\ \rho^- & -\frac{\rho^0}{\sqrt{2}} + \frac{\omega}{\sqrt{2}} & K^{*0} \\ K^{*-} & \bar{K}^{*0} & \phi \end{pmatrix}_\mu. \quad (3)$$

For the coupling constant  $g_\sigma$ , we use the value derived according to the chiral multiplets assumption [37],  $g_\sigma = 0.76$ . The values  $g_V = m_\rho/f_\pi = 5.8$  and  $\beta_V = 0.9$  are obtained from the vector meson dominance [36, 38].

From the Lagrangian, one may derive the  $D\bar{D}$  scattering amplitude and then the effective potentials from the  $\sigma$ ,  $\rho$  and  $\omega$  exchange, which are all Yukawa type

$$\begin{aligned}\mathcal{V}_\sigma(r) &= -\frac{g_\sigma^2}{4\pi r}e^{-m_\sigma r}, \\ \mathcal{V}_\rho(r) &= -3\frac{(\beta_V g_V)^2}{16\pi r}e^{-m_\rho r}, \\ \mathcal{V}_\omega(r) &= -\frac{(\beta_V g_V)^2}{16\pi r}e^{-m_\omega r}.\end{aligned}\quad (4)$$

Here we consider only potentials for the isoscalar  $D\bar{D}$  system. For the isovector case, one changes the factor (-3) in  $V_\rho(r)$  to (+1). So the interaction for the  $I = 0$  system is more attractive.

In principle, one may solve the bound state and the scattering problem by inserting these potentials into the Schrödinger equation directly. However, we will see unphysical results appear because all the mesons are assumed to be pointlike particles. The situation is very similar to the  $N\bar{N}$  case where the very short range interaction is unclear [39]. For the realistic system of composite particles, a form factor at each interacting vertex is necessary. We will use the monopole type form factor

$$F(q) = \frac{\Lambda^2 - m^2}{\Lambda^2 - q^2}, \quad (5)$$

where  $\Lambda \sim 1$  GeV is the cutoff,  $m$  is the exchanged meson mass, and  $q$  is its four-momentum. The improved potentials are [14]

$$\begin{aligned}V_\sigma &= -\frac{g_\sigma^2}{4\pi}\left[\frac{1}{r}(e^{-m_\sigma r} - e^{-\Lambda r}) - \frac{\Lambda^2 - m_\sigma^2}{2\Lambda}e^{-\Lambda r}\right], \\ V_\rho &= -3\frac{(\beta_V g_V)^2}{16\pi}\left[\frac{1}{r}(e^{-m_\rho r} - e^{-\Lambda r}) - \frac{\Lambda^2 - m_\rho^2}{2\Lambda}e^{-\Lambda r}\right], \\ V_\omega &= -\frac{(\beta_V g_V)^2}{16\pi}\left[\frac{1}{r}(e^{-m_\omega r} - e^{-\Lambda r}) - \frac{\Lambda^2 - m_\omega^2}{2\Lambda}e^{-\Lambda r}\right].\end{aligned}\quad (6)$$

Here we use one cutoff to describe the system. The case  $\Lambda \rightarrow \infty$  gives the former potentials. We will call this case the point particle limit.

After one gets the phase shifts with these potentials, the threshold parameters can be derived through the definition

$$\lim_{k \rightarrow 0} k^{2L+1} \cot(\delta_L) \equiv \frac{1}{a_L}, \quad (7)$$

where  $a_0$  ( $a_1$ ) denotes the scattering length (volume) for the S (P)- wave interaction. With this convention,  $a_L$  is negative if the interaction is repulsive. For a system with attractive interactions,  $a_L > 0$  if there is no bound state and  $a_L < 0$  when one bound state appears.

### III. THE S WAVE $D\bar{D}$ SYSTEM

We mainly explore whether there exists an S-wave bound state. From the previous studies [10, 11, 14], we have learned that the numerical results are very sensitive to the cutoff  $\Lambda$ . Since the contact interaction of the form  $\sim \delta(\vec{r})$  does not exist, it is instructive to study the case  $\Lambda \rightarrow \infty$  first. We solve the bound state with the potentials in Eq. (4). The  $\sigma$  meson is a broad scalar resonance with strong coupling to  $I = 0$   $\pi\pi$  S- wave scattering states. Its mass is not definite but around 400~600 MeV [40–42]. We choose two limit cases,  $m_\sigma = 400$  MeV and 600 MeV. Other parameters are  $m_\rho = 775.49$  MeV,  $m_\omega = 782.65$  MeV, and  $m_D = 1867.23$  MeV. If one ignores the vector meson potentials  $\mathcal{V}_\rho$  and  $\mathcal{V}_\omega$  (we label this case NV), there are no binding solutions. After the inclusion of the vector exchange potentials (we label this case VC), we get a very deep bound state with the binding energy around 980 MeV, which indicates this is not a physical solution. A smaller cutoff suppresses the contributions from the short range vector meson interactions. A number around 1 GeV should be reasonable. In the following calculation, we take  $\Lambda = 0.8, 1.0, 1.2, 1.5,$  and  $2.0$  GeV and compare the results (note the lower bound should satisfy  $\Lambda > m_\omega$ ).

We present the calculated S- wave phase shifts of the elastic  $D\bar{D}$  scattering in Fig. 1. In these diagrams,  $E$  is the energy of the  $D$  meson in the center of mass frame. According to the Levinson theorem, the phase shift approaches  $180^\circ$  when  $E \rightarrow 0$  if a bound state exists. The results in the figure indicate that a  $D\bar{D}$  bound state is possible if the

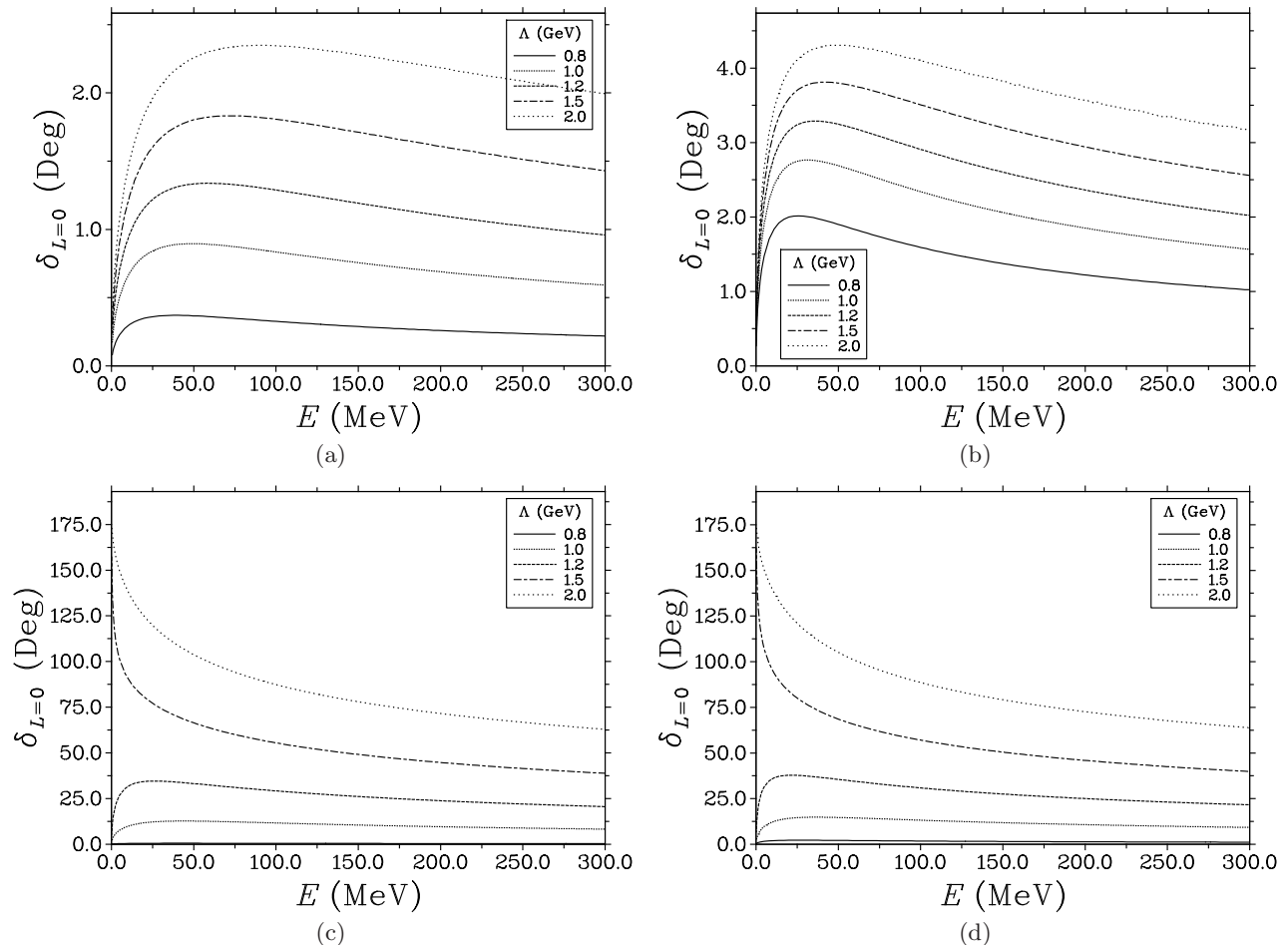


FIG. 1: The phase shifts for the S wave  $D\bar{D}$  scattering with various parameters. The upper (lower) two diagrams correspond to the cases without (with) vector meson exchange contributions. The left (right) two diagrams are obtained with  $m_\sigma=600$  (400) MeV. The cutoff  $\Lambda$  is in units of GeV.

TABLE I: S- wave  $D\bar{D}$  scattering lengths in units of fm. NV (VC) indicates the contributions from vector mesons are omitted (included). The number of \* in the table indicates existence of a bound state. The binding energies are given in Table II.

$m_\sigma$ (MeV)	Vector meson exchange	$\Lambda$ (GeV)					
		0.8	1.0	1.2	1.5	2.0	$\infty$
600	NV	0.0091	0.020	0.027	0.035	0.041	0.051
400	NV	0.064	0.081	0.092	0.10	0.11	0.12
600	VC	0.014	0.31	1.23	-5.46(*)	-1.14 (*)	0.60(*)
400	VC	0.068	0.40	1.56	-4.23(*)	-1.10(*)	0.74(*)

short range attraction is strong, e.g.  $\Lambda \geq 1.5$  GeV. If the cutoff is around 1.2 GeV or less, the S- wave  $D\bar{D}$  bound state does not exist.

With the obtained phase shifts, it is not difficult to derive the S- wave  $D\bar{D}$  scattering lengths. We list them in Table I. The negative scattering lengths suggest that one bound state exists, which can be understood from the diagrams (c) and (d) in Fig. 1. The results for the case  $\Lambda \rightarrow \infty$  are also given in the table. The phase shift goes up from  $180^\circ$  in the case of VC, so the derived scattering length is positive.

We also revisit the bound state problem which was studied in Ref. [14]. The binding energies are summarized in Table II.

It is straightforward to get the S- wave total cross sections from the phase shifts. We present them in Fig. 2. One may check the values at the threshold with the formula  $\sigma_{L=0} = 4\pi a_0^2$ . This explains why the cross section at threshold with  $\Lambda = 2.0$  GeV is smaller than that with  $\Lambda = 1.2$  (or 1.5) GeV in the case of VC.

From the above results, one concludes that an S- wave  $D\bar{D}$  bound state may exist when the short range attraction

TABLE II: The binding energies for the different cases in units of MeV. The three values for the S- wave  $B\bar{B}$  in the case of  $\Lambda \rightarrow \infty$  correspond to the ground state, the first and second radially excited states, respectively.

Systems	$m_\sigma$ (MeV)	$\Lambda$ (GeV)			
		1.2	1.5	2.0	$\infty$
$DD$ (S wave)	600	×	-0.8	-29.4	-974.5
	400	×	-1.4	-31.8	-980.9
$BB$ (S wave)	600	-8.3	-57.4	-186.0	-4916.7 (n=1)
					-444.4 (n=2)
					-1.3 (n=3)
	400	-10.1	-60.7	-190.5	-4924.8 (n=1)
					-449.7 (n=2)
					-2.0 (n=3)
$BB$ (P wave)	600	×	×	×	-377.4
	400	×	×	-0.6	-383.1

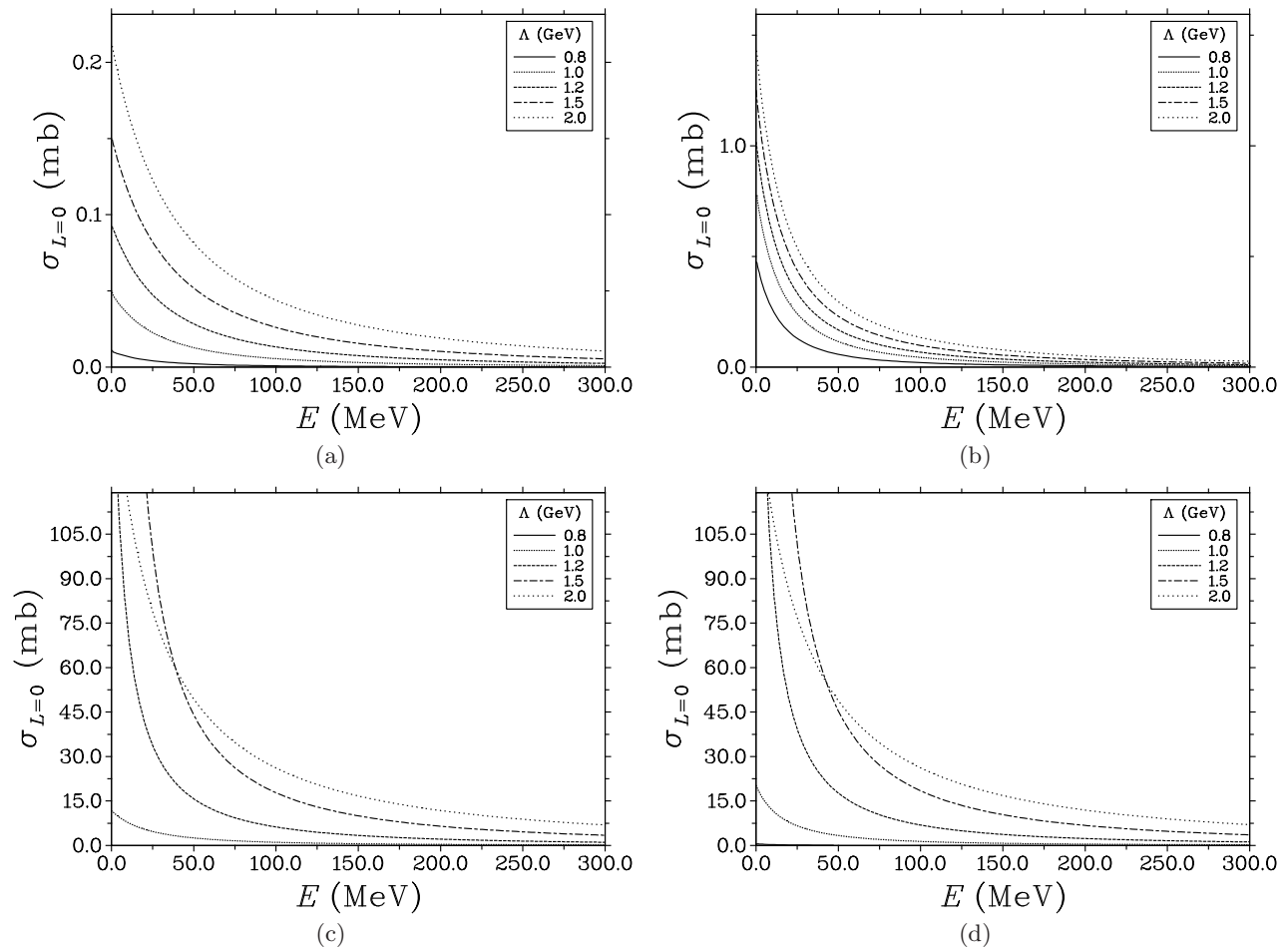


FIG. 2: The S- wave total cross sections for the  $D\bar{D}$  scattering with various parameters. The upper (lower) two diagrams correspond to the cases without (with) vector meson exchange contributions. The left (right) two diagrams are obtained with  $m_\sigma=600$  (400) MeV. The cutoff  $\Lambda$  is in units of GeV.

is strong. Unfortunately the behavior of the short range interaction is not completely understood. Whether the vector meson exchange interaction is important, or equivalently whether  $\Lambda$  is large, needs further study. The determination of a reasonable range for this parameter is one major task in this framework.  $\Lambda \rightarrow \infty$  is not a realistic case because the binding energy around 1 GeV is too large to be explained by the  $\rho$  and  $\omega$  meson exchanges. In fact, if this is the case, the  $D\bar{D}$  bound state is so compact that it should be represented by a 4-quark system, and it is not consistent with the  $D\bar{D}$  molecular state. In the cases of a finite cutoff, a value larger than 2.0 GeV will lead to the binding

energy more than 30 MeV while that around 1.2 GeV does not result in a binding solution. However, it is difficult to identify the reasonable range without further information. The extraction of the scattering length from lattice QCD simulations or experimental measurements will be helpful. One will see that the P- wave  $B\bar{B}$  production is another observable to constrain the range of  $\Lambda$ . We will come back to this point later.

#### IV. THE P-WAVE $D\bar{D}$ SYSTEM

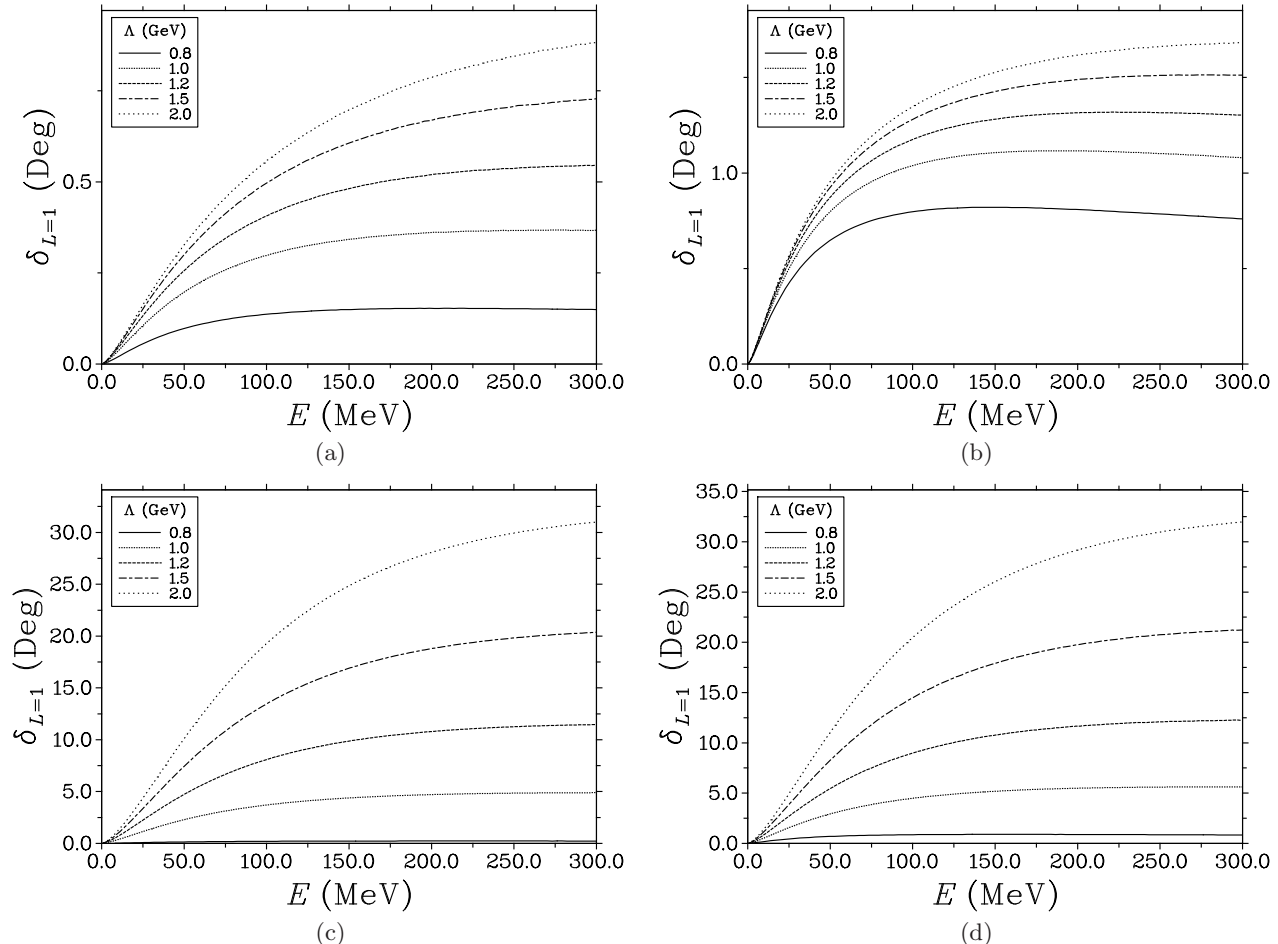


FIG. 3: The phase shifts for the P- wave  $D\bar{D}$  scattering with various parameters. The upper (lower) two diagrams correspond to the cases without (with) vector meson exchange contributions. The left (right) two diagrams are obtained with  $m_\sigma=600$  (400) MeV. The cutoff  $\Lambda$  is in units of GeV.

TABLE III: The P- wave  $D\bar{D}$  scattering volumes in units of  $\text{fm}^3$ . NV (VC) indicates the contributions from vector mesons are omitted (included).

$m_\sigma$ (MeV)	Vector meson exchange	$\Lambda$ (GeV)					
		0.8	1.0	1.2	1.5	2.0	$\infty$
600	NV	0.0014	0.0024	0.0029	0.0032	0.0033	0.0034
400	NV	0.015	0.016	0.017	0.017	0.017	0.017
600	VC	0.0019	0.023	0.041	0.058	0.070	0.085
400	VC	0.015	0.037	0.055	0.072	0.087	0.10

The P-wave centrifugal barrier makes the interaction weaker than that in the S-wave case. Actually, we do not find any binding solutions even in the point particle limit ( $\Lambda \rightarrow \infty$ ). In Fig. 3, we show the phase shifts derived with different parameters. The diagrams indicate that the attraction is not strong enough to form a bound state

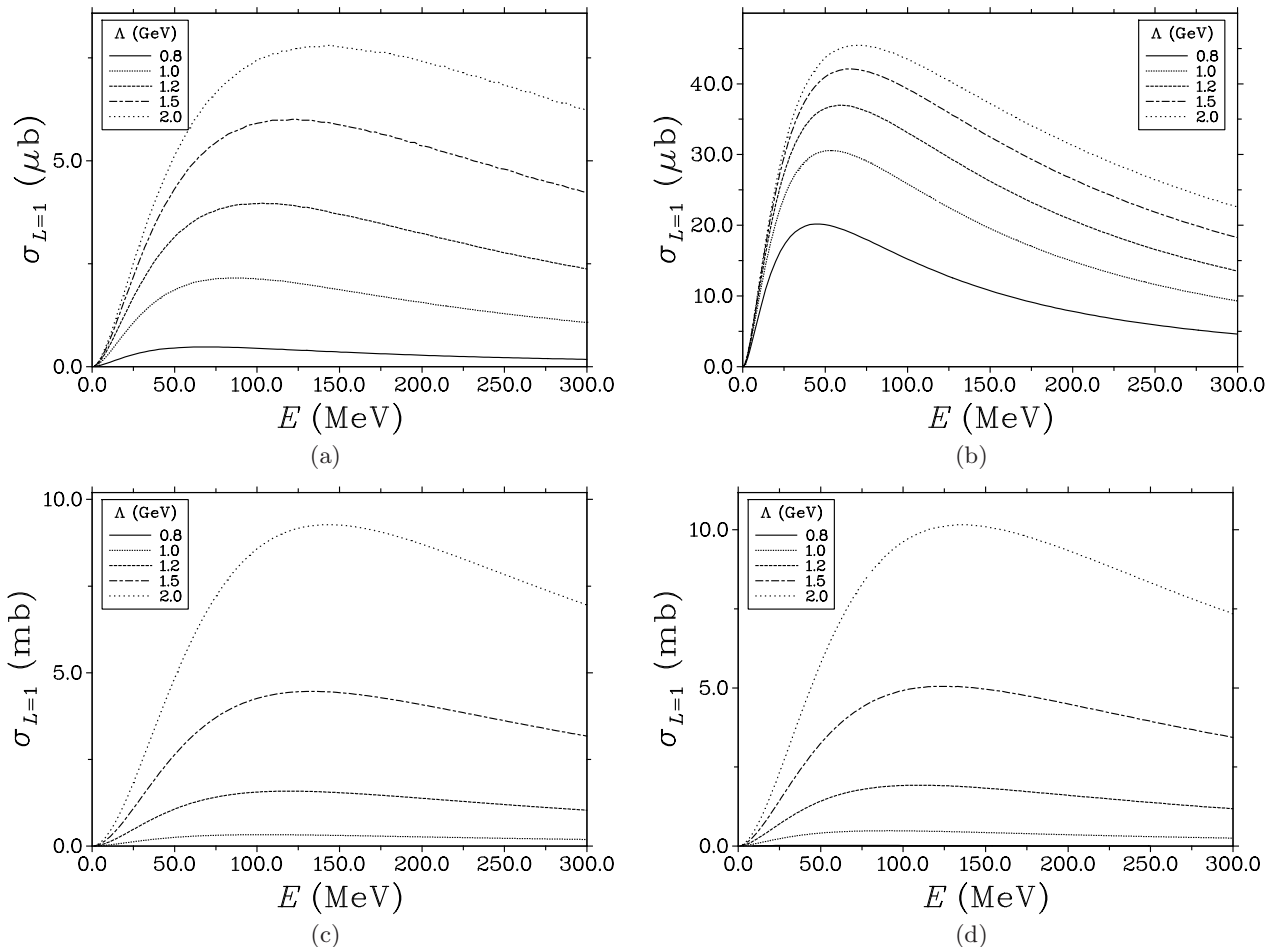


FIG. 4: The P- wave total cross sections for the  $D\bar{D}$  scattering with various parameters. The upper (lower) two diagrams correspond to the cases without (with) vector meson exchange contributions. The left (right) two diagrams are obtained with  $m_\sigma=600$  (400) MeV. The cutoff  $\Lambda$  is in units of GeV.

nor a resonance. Similar to the S- wave case, one may get the scattering volumes from the phase shifts according to the definition Eq. (7). We present the numerical results in Table III. The stronger the attraction is, the larger the scattering volume becomes. The obtained P- wave scattering cross sections are shown in Fig. 4.

It is very interesting to note that there is a resonancelike structure or bump in the cross section, although no bound state or resonance pole (where the scattering phase shift crosses  $90^\circ$ ) exists in this channel. The structure appears when the total energy of motion is around 40~150 MeV, depending on the parameters. The P- wave interaction probably has effects on the production of  $\psi(3770)$  or  $D\bar{D}$ . We will explore this issue in the following section.

To compare with the future experimental measurements of the scattering cross sections, one has to sum up different partial wave contributions. Here we have performed the calculation up to P wave since the higher partial waves yield smaller contributions. Because the S- wave cross section is much larger than the P- wave one, the total line shape of the cross sections  $\sigma_{tot} = \sigma_{L=0} + \sigma_{L=1}$  is similar to that of the S- wave case. That is, the resonancelike structure of the P- wave interaction does not appear in the total cross section.

## V. THE RESCATTERING EFFECT IN $e^+e^- \rightarrow D\bar{D}$ PRODUCTION

### A. Formulation

The above P- wave structure motivates us to calculate the  $D\bar{D}$  production by including their rescattering effect, which may be helpful to understand the anomalous line shapes observed by the BES Collaboration [27, 28]. The schematic diagram for this effect in the process  $e^+e^- \rightarrow D\bar{D}$  is plotted in Fig. 5. The  $D\bar{D}$  pair comes mainly from

$\psi(3770)$ . In a previous work [34], the production near the threshold has been studied by including the single loop contributions of the intermediate  $D\bar{D}$ ,  $D\bar{D}^* + c.c.$ , and  $D^*\bar{D}^*$ . In this work, we would like to consider the multiple rescattering effects using a nonrelativistic method.

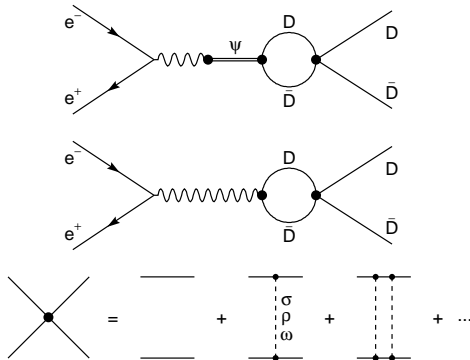


FIG. 5: The rescattering effects in the  $D\bar{D}$  production process.

One may find the detailed procedure to derive the formula in the Appendix A. Here, we only present the resultant production cross section  $\sigma_{prod} = \sigma_1 + \sigma_2$ . The first part gives the cross section without FSI,

$$\sigma_1 = \frac{\pi}{3} \alpha_e^2 \frac{(s - 4m_D^2)^{3/2}}{s^{5/2}} \times |\text{f.f.}|^2, \quad (8)$$

where  $\alpha_e = 1/137$  and f.f. indicates the contributions from intermediate vector resonances and background fields [34, 43, 44]. Since we here focus only on the illustration of FSI effect in the following analysis, we consider one resonance  $\psi(3770)$  and take simply the form of f.f. from Ref. [43],

$$\text{f.f.} = -F_{D\bar{D}}(s) + \frac{g_{\psi D\bar{D}} Q_c f_\psi m_\psi}{s - m_\psi^2 + im_\psi \Gamma_T} e^{i\phi}, \quad (9)$$

where the coupling  $g_{\psi D\bar{D}}$  is defined through  $\langle D(p_1)\bar{D}(p_2)|\psi(p, \lambda) \rangle = -ig_{\psi D\bar{D}} \epsilon^{(\lambda)} \cdot (p_1 - p_2)(2\pi)^4 \delta^4(p - p_1 - p_2)$ ,  $Q_c$  is the electric charge of the charm quark, the decay constant  $f_\psi$  of  $\psi(3770)$  is given by  $\langle 0|\bar{c}\gamma_\mu c|\psi(\lambda) \rangle = f_\psi m_\psi \epsilon_\mu^{(\lambda)}$ ,  $m_\psi$  ( $\Gamma_T$ ) is the mass (width) of  $\psi(3770)$ ,  $\phi$  is a relative phase, and  $F_{D\bar{D}}(s)$  is an effective form factor describing the coupling of the virtual photon with the  $D\bar{D}$  pair. Here, we assume

$$F_{D\bar{D}}(s) = \frac{m_\psi^2 F_0}{s} \quad (10)$$

with  $F_0$  as an adjustable constant [43]. One derives  $g_{\psi D\bar{D}}$  from the branching ratio of the strong decay and  $f_\psi$  from the leptonic decay width  $\Gamma_{ee}$ . Note one should consistently consider the rescattering effect in determining  $g_{\psi D\bar{D}}$  from the  $\psi(3770)$  decay. Now the decay width also has two parts  $\Gamma = \Gamma_1 + \Gamma_2$ . We have  $\Gamma_2/\Gamma_1 = \sigma_2/\sigma_1$  at the peak  $\sqrt{s} = m_\psi$ .

The second part reflects the rescattering effect

$$\sigma_2 = \frac{64 \pi^2 \alpha_e^2 \lambda}{9 s^2 m_D} \left\{ \frac{2(\text{Re}U \times \text{Im}U)W^r - [(\text{Re}U)^2 - (\text{Im}U)^2]W^i}{(W^r)^2 + (W^i)^2} \right\} \times |\text{f.f.}|^2. \quad (11)$$

We have adopted the Yamaguchi separable potential approximation [35] in deriving this formula and  $\lambda$  is the coupling



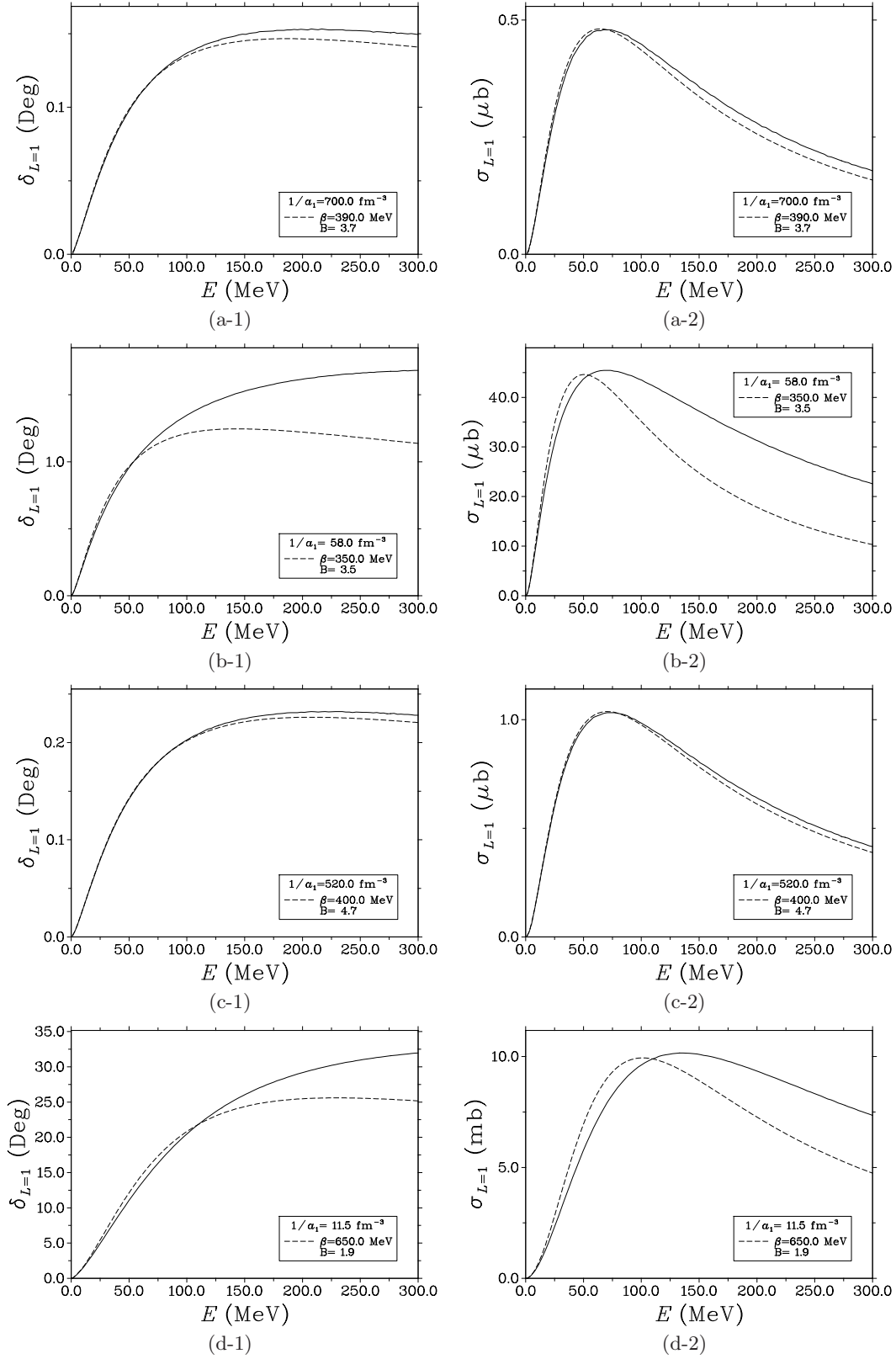


FIG. 6: The reproduced P- wave  $DD\bar{D}$  phase shifts  $\delta_{L=1}$  and cross sections  $\sigma_{L=1}$  in the four cases, (a):  $1/a_1=700.0 \text{ fm}^{-3}$ , (b):  $1/a_1=58.0 \text{ fm}^{-3}$ , (c):  $1/a_1=520.0 \text{ fm}^{-3}$ , and (d):  $1/a_1=11.5 \text{ fm}^{-3}$ , respectively. The solid line denotes the results calculated in the former section.

constant. This approximation has recently been used to study the structure of X(3872) [45]. In the above formula,

$$ReU = -m_D^2 \frac{\beta}{2\pi^2} \mathcal{P} \int_0^\infty dk \frac{k^4}{(k^2 + 2M^2)(k^2 - \alpha^2)} t(k) F_p(k), \quad (12)$$

$$ImU = -m_D \frac{\beta \alpha^3}{4\pi \sqrt{s}} t(\alpha) F_p(\alpha), \quad (13)$$

$$W^r = 1 - \frac{\lambda \beta^2}{6\pi^2} \mathcal{P} \int_0^\infty dk \frac{k^4}{k^2 - \alpha^2} [t(k)]^2, \quad (14)$$

$$W^i = -\frac{\lambda \beta^2 \alpha^3}{12\pi} [t(\alpha)]^2, \quad (15)$$

$$t(k) = \frac{1}{(k^2 + \beta^2)^2} + \frac{B}{\beta^2(k^2 + \beta^2)}, \quad (16)$$

where  $\alpha^2 \equiv m_D(\sqrt{s} - 2m_D)$  and  $\mathcal{P}$  means the principal value integration. We will determine  $\lambda$ ,  $\beta$ , and  $B$  by reproducing the phase shifts and the scattering cross section calculated in the previous section (see Appendix B). We have introduced a phenomenological form factor in the  $D\bar{D}$  production vertex

$$F_p(k) = \frac{\Lambda_p^2}{\Lambda_p^2 + k^2}, \quad (17)$$

where the cutoff  $\Lambda_p$  around 1 GeV reflects the loop contributions in considering rescattering effects. Here,  $k$  means the virtuality and the coupling between  $\psi(3770)$  and  $D\bar{D}$  becomes small when the virtuality of the  $D$  meson is large. This form factor helps to derive a physically reasonable  $g_{\psi D\bar{D}}$ , which will be obtained with the following expression:

$$Br(\psi(3770) \rightarrow D\bar{D}) \cdot \Gamma_T = g_{\psi D\bar{D}}^2 \left\{ \frac{(m_\psi^2 - 4m_D^2)^{3/2}}{24\pi m_\psi^2} + \frac{8}{9} \frac{\lambda}{m_D m_\psi} \left[ \frac{2(ReU \times ImU)W^r - [(ReU)^2 - (ImU)^2]W^i}{(W^r)^2 + (W^i)^2} \right]_{\sqrt{s}=m_\psi} \right\}. \quad (18)$$

## B. Results

We choose four cases of parameters to compare with each other: (a)  $m_\sigma = 600$  MeV,  $\Lambda = 0.8$  GeV, and NV; (b)  $m_\sigma = 400$  MeV,  $\Lambda = 2.0$  GeV, and NV; (c)  $m_\sigma = 600$  MeV,  $\Lambda = 0.8$  GeV, and VC; and (d)  $m_\sigma = 400$  MeV,  $\Lambda = 2.0$  GeV, and VC. The first case has the weakest attraction, while the fourth one has the strongest attraction.

For the case (a), we have  $1/a_1 = 700.0 \text{ fm}^{-3}$ . We found  $(\beta, B) = (370, 8.5), (380, 5.2), (390, 3.7), (400, 2.7), (410, 2.2)$  [the unit of  $\beta$  is MeV] can all roughly reproduce the cross sections and the phase shifts. We take  $\beta = 390$  MeV,  $B = 3.7$  as an example to illustrate the result. The reproduced phase shifts and cross sections are presented in Fig. 6(a) and the calculated production cross sections are given in Fig. 7(a). We also put the BES data [28] in the diagram. When plotting the latter diagram, we have used:  $\Lambda_p = 1.0$  GeV,  $m_\psi = 3772.92$  MeV [46],  $\Gamma_T = 27.3$  MeV [46],  $f_\psi = 100.4$  MeV obtained from  $\Gamma_{ee} = 0.265$  keV [46],  $g_{\psi D\bar{D}} = 12.6$  from  $Br(\psi(3770) \rightarrow D\bar{D}) = 0.853$  [46],  $F_0 = 5.0$  and  $\phi = \pi/2$ . One finds that the FSI contribution is small in this case, and it certainly does not lead to an anomalous line shape.

For the case (b), we have  $1/a_1 = 58.0 \text{ fm}^{-3}$ . The parameters may be  $(\beta \text{ (MeV)}, B) = (320, 30), (330, 10), (340, 5.5), (350, 3.5), (360, 2.7), (370, 2.0),$  or  $(380, 1.6)$ . As an example, we present the phase shifts and cross sections corresponding to  $\beta = 350$  MeV,  $B = 3.5$  in Fig. 6(b) and the calculated production cross sections in Fig. 7(b). Now the coupling constant becomes  $g_{\psi D\bar{D}} = 11.9$ , while the other parameters are unchanged. The attraction is stronger, but the line shape is still normal.

For the case (c),  $1/a_1 = 520.0 \text{ fm}^{-3}$ . The values  $(\beta, B) = (370, 50), (380, 13), (390, 7.0), (400, 4.7), (410, 3.5), (420, 2.6), (430, 2.1),$  or  $(450, 1.4)$  are acceptable where the unit of  $\beta$  is MeV. With  $\beta = 400$  MeV,  $B = 4.7$ , the fitted phase shifts and cross sections are plotted in Fig. 6(c). We present the calculated production cross sections in Fig. 7(c). In this case, we have the same coupling constant  $g_{\psi D\bar{D}} = 12.6$  as case (a). Because the contributions from the vector meson exchange interactions are small, the line shape is also similar.

For the case (d), with  $1/a_1 = 11.5 \text{ fm}^{-3}$ , one may use  $(\beta, B) = (550, 60), (570, 12), (590, 5.8), (600, 4.5), (650, 1.9), (700, 1.0),$  or  $(800, 0.2)$  to reproduce the phase shifts and the cross sections. Figure 6(d) shows an illustration with

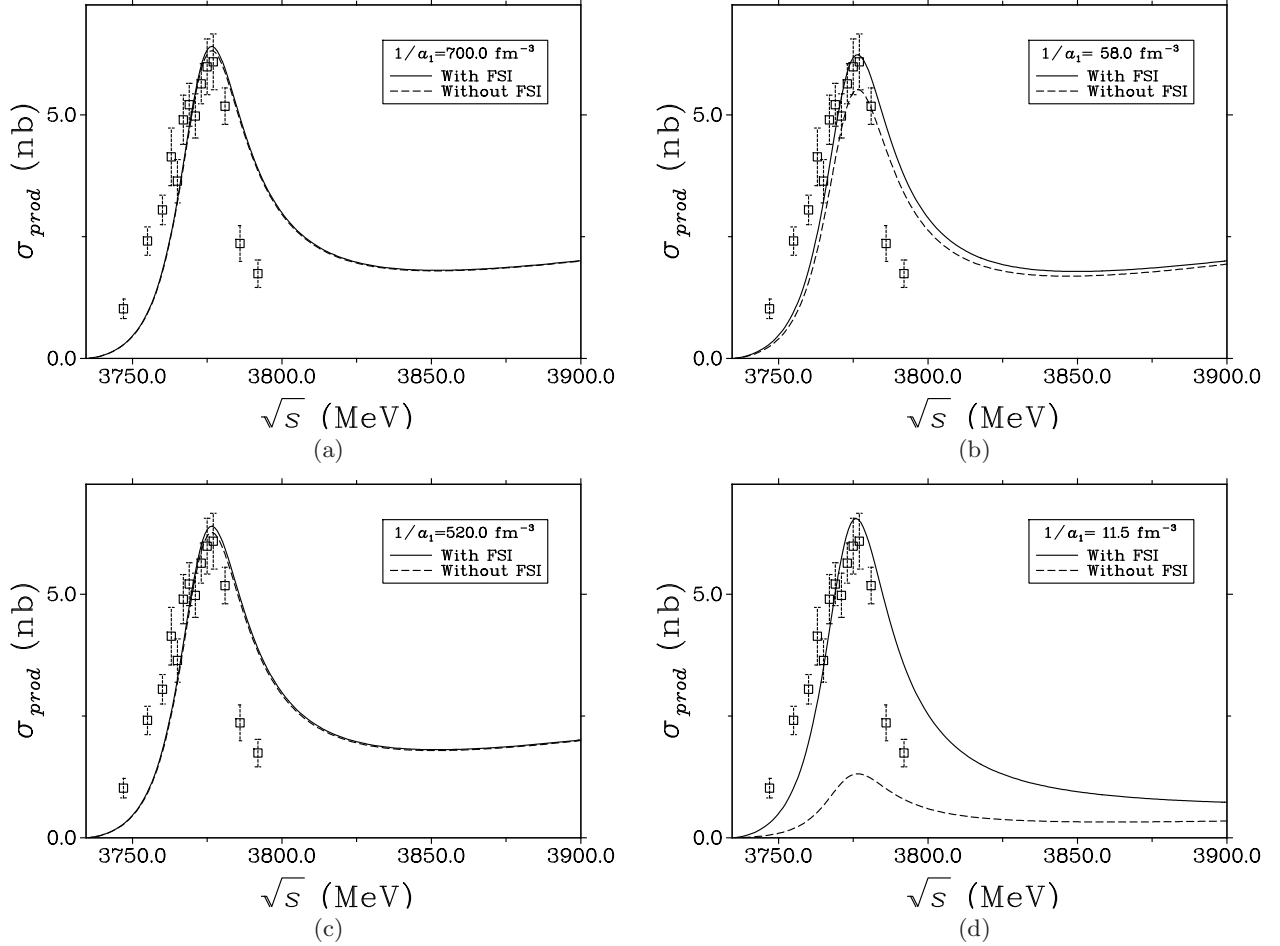


FIG. 7: The obtained  $D\bar{D}$  production cross sections correspond to the four cases (a):  $1/a_1=700.0 \text{ fm}^{-3}$ , (b):  $1/a_1=58.0 \text{ fm}^{-3}$ , (c):  $1/a_1=520.0 \text{ fm}^{-3}$ , and (d):  $1/a_1=11.5 \text{ fm}^{-3}$ , respectively. We get the dash lines by ignoring the rescattering part  $\sigma_2$  of the production cross section  $\sigma_{prod} = \sigma_1 + \sigma_2$ . The experimental data are taken from Ref. [28].

$\beta = 650 \text{ MeV}$  and  $B=1.9$ . We plot the corresponding production cross section in the last diagram of Fig. 7. Now two parameters have been changed:  $g_{\psi D\bar{D}} = 5.6$  and  $F_0 = 2.0$ . For the other combinations of  $\beta$  and  $B$ , the magnitude changes a little but it can be adjusted to the experimental data by varying  $F_0$  and the phase angle  $\phi$ . Although the final state attraction is strong, the anomalous line shape does not appear even in this case.

The results of these four cases (Fig. 7) tell us that the  $D\bar{D}$  rescattering effects cannot change the line shape of the production cross section. The reason is that the P- wave interaction is still not attractive enough. To see a cross section of a stronger attraction, let us arbitrarily consider an extreme case:  $1/a_1 = 0.5 \text{ fm}^{-3}$ ,  $\beta=500.0 \text{ MeV}$ , and  $B=0.0$ , where no bound state or resonance pole is formed, though a sharp rise of the P-wave phase shift is observed just above the threshold. The corresponding phase shifts and the resulting  $D\bar{D}$  production cross sections are plotted in Fig. 8. We have used  $g_{\psi D\bar{D}} = 4.6$  and  $F_0 = 1.5$ . One finds that the anomalous line shape appears now. Also, the peak around  $3770 \text{ MeV}$  is shifted to a little lower position. The fact that the FSI may lower the mass of a bound state or a resonance reflects the couple channel effects. Because the scattering volume is much larger than the maximum number  $0.1 \text{ fm}^3$  in Table III, this case may not be realistic.

From the above results, we conclude that although the strong FSI may lead to anomalous line shapes in the production processes in the unrealistic case, one cannot interpret those observed by the BES Collaboration with this mechanism. It is worthwhile to study further whether the anomalous line shapes are due to other nearby resonances, new resonances, or channel coupling effects.

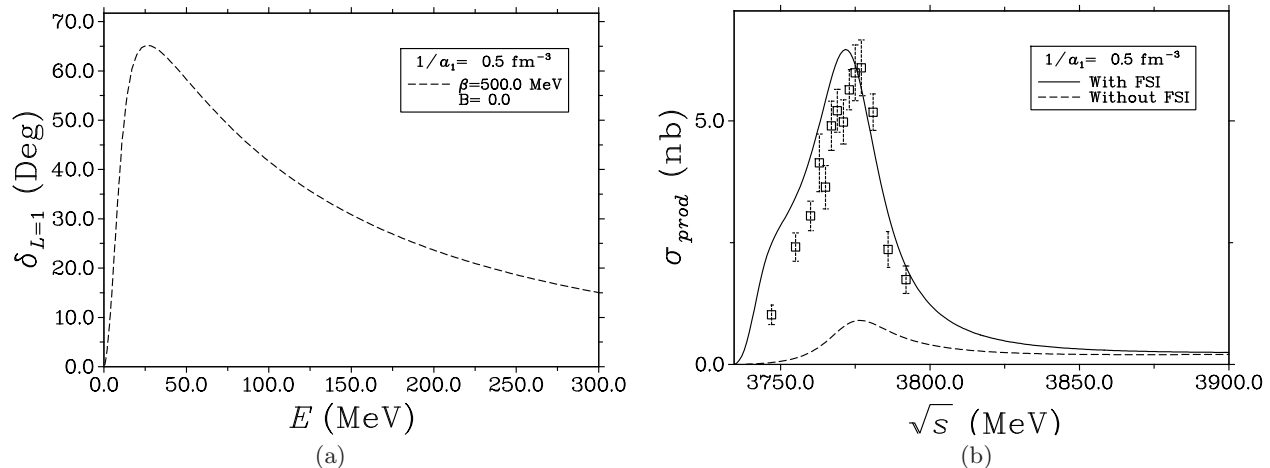


FIG. 8: The P- wave  $D\bar{D}$  phase shifts (a) and their production cross section (b) in an extreme case with  $1/a_1=0.5 \text{ fm}^{-3}$ ,  $\beta=500 \text{ MeV}$  and  $B=0$ . We get the dash line in the right diagram by ignoring the rescattering part  $\sigma_2$  of the production cross section  $\sigma_{prod} = \sigma_1 + \sigma_2$ . The experimental data are taken from Ref. [28].

## VI. THE $B\bar{B}$ SYSTEM

All the previous studies may be extended to the  $B\bar{B}$  case naturally. Now  $\Upsilon(4S)$  is slightly above the threshold. The features, in principle, should be similar to those of the  $D\bar{D}$  case. But we will see more interesting results. We will present the figures only if the line shape is strange. When performing the numerical evaluation, the new parameters we have to use are the meson masses [46]  $m_B = 5279.34 \text{ MeV}$ ,  $m_\Upsilon = 10579.4 \text{ MeV}$ , the width [46]  $\Gamma_T = 20.5 \text{ MeV}$  and  $\Gamma_{ee} = 0.272 \text{ keV}$ , the branching ratio  $B_r(\Upsilon(4S) \rightarrow B\bar{B}) = 0.96$ , the derived decay constant  $f_\Upsilon = 340.7 \text{ MeV}$ , and the electric charge of the heavy quark  $Q_b = -1/3$ . The derived coupling constant without FSI is  $g_{TB\bar{B}} = 23.9$ . We adopt a little larger cutoff  $\Lambda_p=1.1 \text{ GeV}$  for this case.

TABLE IV: The S- wave  $B\bar{B}$  scattering lengths in unit of fm. NV (VC) indicates the contributions from vector mesons are omitted (included). The number of \* in the table indicates that of the binding solutions. The binding energies are given in Table II.

$m_\sigma$ (MeV)	Vector meson exchange	$\Lambda$ (GeV)					
		0.8	1.0	1.2	1.5	2.0	$\infty$
600	NV	0.026	0.058	0.083	0.11	0.13	0.17
400	NV	0.19	0.26	0.30	0.34	0.38	0.44
600	VC	0.039	2.74	-1.32(*)	-0.46(*)	1.08(*)	-3.02(***)
400	VC	0.21	7.47	-1.22(*)	-0.38(*)	1.76(*)	-2.56(***)

The S- wave  $B\bar{B}$  bound state is more likely to exist than the  $D\bar{D}$  one. Our calculated phase shifts do not exceed  $16^\circ$  when one considers only the scalar meson exchange contribution, which indicates there is no bound state. After one includes the vector meson contributions, the phase shift starts from  $180^\circ$  with a cutoff  $\Lambda=1.2 \text{ GeV}$ . It can go up to  $210^\circ$  from  $180^\circ$  with a stronger attraction  $\Lambda = 2.0 \text{ GeV}$ . We present the derived scattering lengths in Table IV and the binding solutions in Table II. In the point particle limit, the observation that three solutions exist and that the binding energies are large indicates this case is not physical once again. A finite reasonable cutoff should be slightly larger than that in the  $D\bar{D}$  case because of the heavy quark symmetry and the smaller size of the  $B$  meson. As for  $\Lambda=2.0 \text{ GeV}$  and VC, the scattering phase shift crosses  $\delta_{L=0} = \pi$  at a finite  $E$  and therefore the S-wave cross section becomes zero at that point.

For the P- wave interactions, we show the phase shifts with various parameters in Fig. 9. It can reach  $180^\circ$  with a strong attraction, e.g.  $\Lambda = 2.0 \text{ GeV}$ ,  $m_\sigma = 400 \text{ MeV}$  and VC. Note the line for  $\Lambda = 2.0 \text{ GeV}$  in the diagram in Fig. 9(c) is a resonance while that in the diagram in Fig. 9(d) is a bound state. Therefore, the results are more interesting than that in the  $D\bar{D}$  case. We give the derived scattering volumes in Table V and the binding solutions in Table II. In the point particle limit, the positive scattering volume and the existence of one binding solution come from the observation that the phase shift goes up to  $\sim 245^\circ$  from  $180^\circ$ . The large binding energies in this limit again require a finite cutoff. If the cutoff less than  $1.5 \text{ GeV}$  is reasonable, then no P- wave binding solutions exist. We present the cross sections for different parameters in Fig. 10. Comparing this figure with Fig. 4, one observes the resonancelike

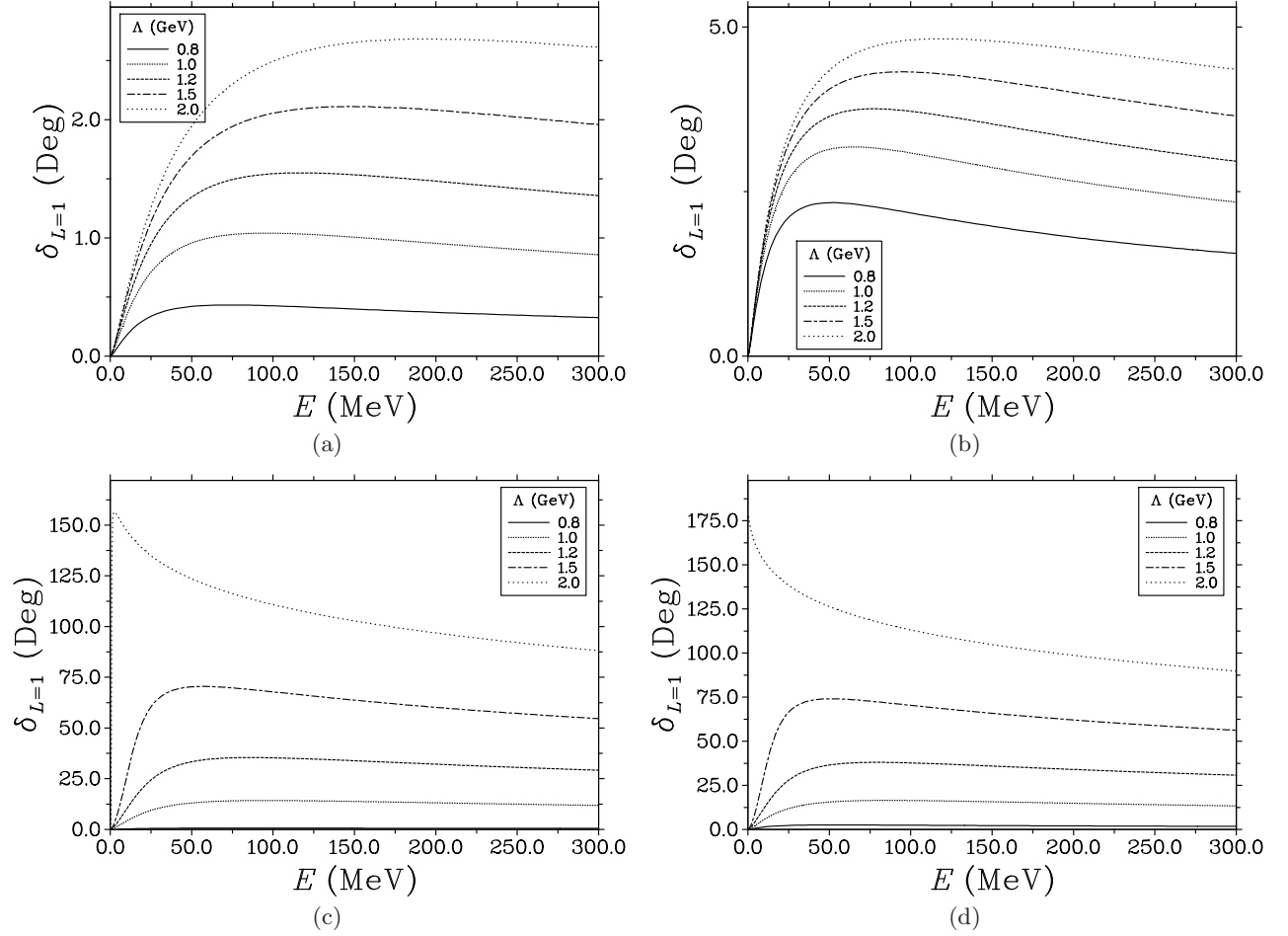


FIG. 9: The phase shifts for the P- wave  $B\bar{B}$  scattering with various parameters. The upper (lower) two diagrams correspond to the cases without (with) vector meson exchange contributions. The left (right) two diagrams are obtained with  $m_\sigma=600$  (400) MeV. The cutoff  $\Lambda$  is in units of GeV.

TABLE V: The P- wave  $B\bar{B}$  scattering volumes in unit of  $\text{fm}^3$ . NV (VC) indicates the contributions from vector mesons are omitted (included). The number of \* in the table indicates that of the binding solutions. The binding energies are given in Table II.

$m_\sigma$ (MeV)	Vector meson exchange	$\Lambda$ (GeV)					
		0.8	1.0	1.2	1.5	2.0	$\infty$
600	NV	0.0040	0.0067	0.0083	0.0092	0.0096	0.0099
400	NV	0.042	0.047	0.048	0.050	0.050	0.050
600	VC	0.0054	0.069	0.14	0.26	4.55	0.1~0.2(*)
400	VC	0.043	0.11	0.19	0.34	-5.56(*)	0.2~0.3(*)

structure is more evident. It appears at a smaller energy of motion. Note that the cross section for the case  $\Lambda = 2.0$  GeV (c) also vanishes in the limit  $E = 0$ , which is understood with Eq. (B7) and the nonzero  $1/a_1$ .

To get the total cross section, we have to sum up all the partial wave contributions. In the  $D\bar{D}$  case, the estimated maximum partial wave was  $l_{max} \approx \frac{\sqrt{m_D E}}{m_\sigma} \approx 1.87$ , so we calculated up to P wave. However, in the  $B\bar{B}$  case, one should consider higher partial wave contributions (up to F wave) since  $l_{max} \approx 3.1$ . For the D- wave scattering, the line shapes look like those in the P- wave  $D\bar{D}$  case, but the phase shift can go up to  $100^\circ$  with  $m_\sigma=400$  MeV,  $\Lambda \rightarrow \infty$ , and VC. For a finite cutoff  $\Lambda \leq 2.0$  GeV, a resonancelike structure also appears in the cross sections, although the phase shift does not exceed  $90^\circ$ . The phase shifts for the F- wave scattering do not exceed  $40^\circ$  even in the point particle limit. After summing up these four partial wave contributions, we get the total cross sections shown in Fig. 11. An interesting structure is there if one does not ignore the vector meson exchange contributions. The bump structure for the case  $\Lambda = 1.5$  GeV comes mainly from the P- wave scattering.

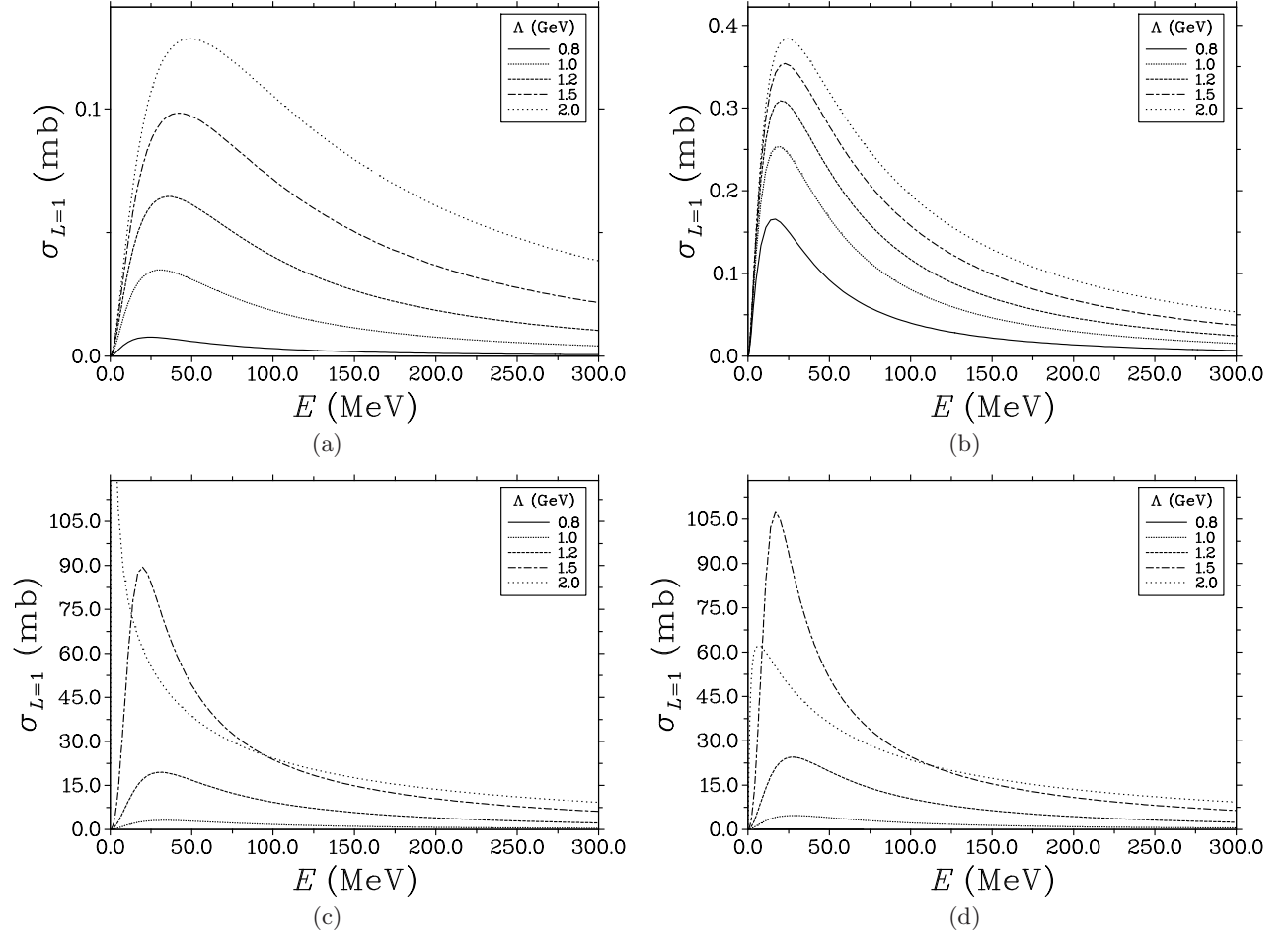


FIG. 10: The P- wave total cross sections for the  $B\bar{B}$  scattering with various parameters. The upper (lower) two diagrams correspond to the cases without (with) vector meson exchange contributions. The left (right) two diagrams are obtained with  $m_\sigma=600$  (400) MeV. The cutoff  $\Lambda$  is in units of GeV.

Now we move on to the final state rescattering effects in the process  $e^+e^- \rightarrow B\bar{B}$ . One may still choose the four cases in the  $D\bar{D}$  system. However, there are no strange line shapes in the cases (a), (b), and (c). Since both a resonance and a bound state are possible in the P- wave scattering with a finite cutoff, here we consider the case (d):  $m_\sigma = 400$  MeV,  $\Lambda = 2.0$  GeV, and VC; case (e):  $m_\sigma = 600$  MeV,  $\Lambda = 2.0$  GeV, and VC; and an extreme case.

For the case (d), we have  $1/a_1 = -0.18 \text{ fm}^{-3}$ . We illustrate the results with  $\beta = 1200$  MeV and  $B = 0.7$ . Figure 12 shows the reproduced phase shifts and cross sections while Fig. 13 shows the calculated production cross sections. We have adopted the coupling  $g_{\Upsilon B\bar{B}} = 3.5$  and the  $D\bar{D}$  parameters  $F_0 = 2.0$  and  $\phi = \pi/2$ . The anomalous line shape reflects the P- wave  $B\bar{B}$  bound state. For the case (e), we plot, with  $1/a_1 = 0.22 \text{ fm}^{-3}$ ,  $g_{\Upsilon B\bar{B}} = 3.0$ ,  $\beta = 1000$  MeV, and  $B = 3.0$ , the reproduced phase shifts and scattering cross sections in Fig. 12 and the corresponding production cross sections in Fig. 13. One should note the production cross section vanishes at the threshold. So we have two peaks in the second diagram of Fig. 13. The sharp one near the threshold is due to a P- wave resonance. Similar to the  $D\bar{D}$  case, we also consider an extreme case:  $1/a_1 = 0.5 \text{ fm}^{-3}$ ,  $\beta = 500$  MeV and  $B = 0$ . Figure 14 displays the derived phase shifts and the obtained production cross sections where  $g_{\Upsilon B\bar{B}} = 11.3$  has been used. Now the anomalous structure is just a bump. The peaks of  $\Upsilon(4S)$  in these cases are shifted to a lower position because of the strong final state interactions.

The big difference between the two diagrams in Fig. 13 results from the fact that the coupling constant in the separable approximation is sensitive to the scattering volume. To see the behavior of the line shape in the separable approximation, let us go to Eq. (B5). From that equation, the coupling is stronger with a bigger value of the scattering volume. If the scattering volume is positive, this indicates that the stronger the  $B\bar{B}$  interaction is, the more obvious the anomalous line shape is. On the other hand, if the scattering volume is negative, the weaker the  $B\bar{B}$  interaction is, the more obvious the anomalous line shape is. Therefore, if there is a sharp P- wave resonance or a shallow P-

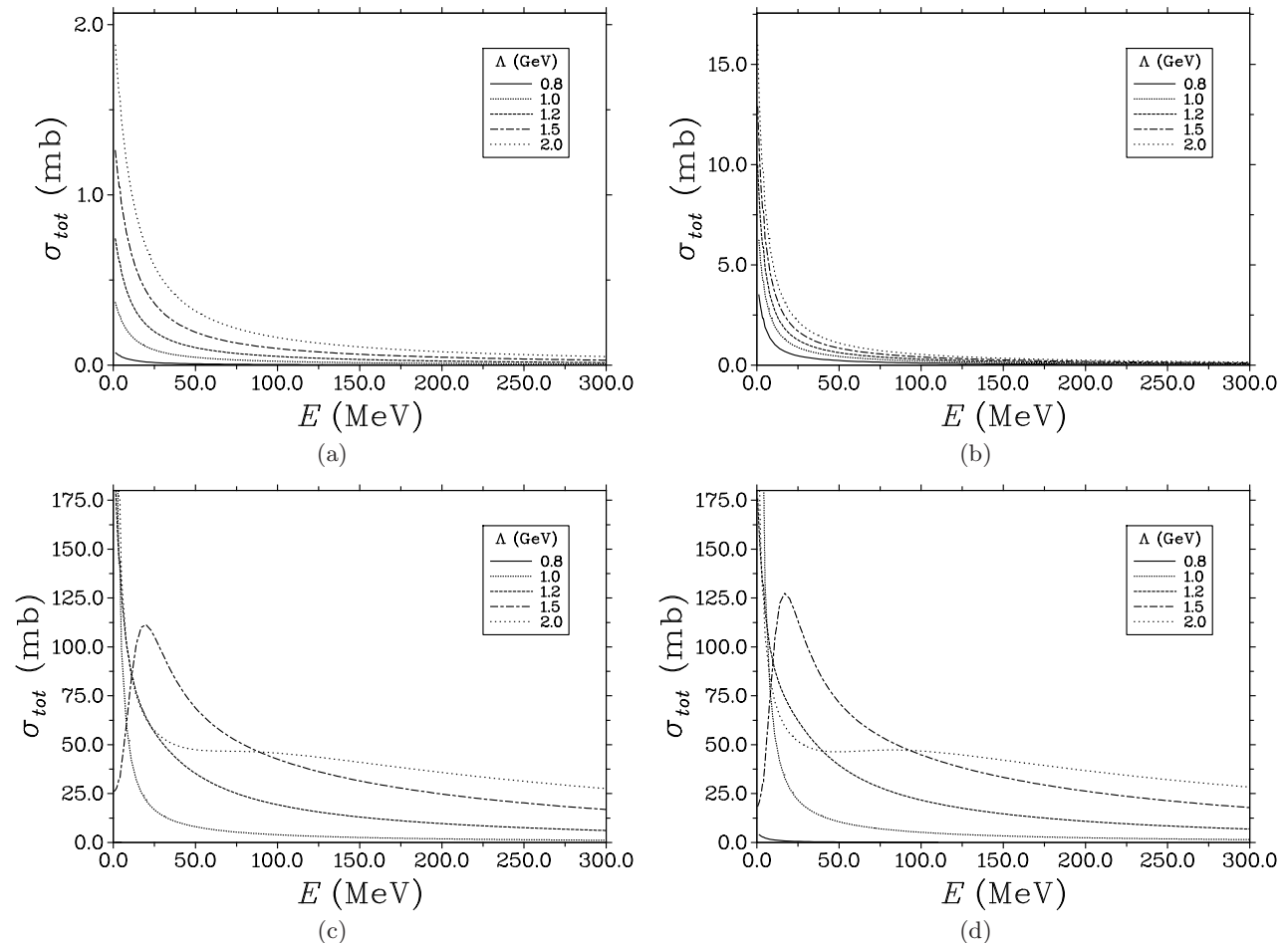


FIG. 11: The total cross sections for the  $B\bar{B}$  scattering with various parameters. The upper (lower) two diagrams correspond to the cases without (with) vector meson exchange contributions. The left (right) two diagrams are obtained with  $m_\sigma=600$  (400) MeV. The cutoff  $\Lambda$  is in units of GeV.

wave bound state around the  $B\bar{B}$  threshold, the structure may be observable in  $e^+e^- \rightarrow B\bar{B}$ . The sensitivity to the scattering volume explains why the two diagrams in Fig. 13 look so different. Since the value is positive for a resonance, the peak is clearer. In one word, the scattering volume mainly affects the line shape of the production cross section. The other two parameters  $\beta$  and  $B$  mainly control the magnitude of the cross section. But then one may recover roughly the same cross section by adjusting  $F_0$  and  $\phi$ .

In Ref. [47], the BaBar Collaboration measured  $R_b(s) = \sigma_b(s)/\sigma_{\mu\mu}(s)$ . One may derive a cross section around 1.2 nb near  $\Upsilon(4S)$  while our result is around 2 nb. The reason may be that we considered only one resonance contribution. The interference between nearby resonances may reduce this number [44]. The normal line shape of the BaBar data tells us that the above three cases are not realistic, which means the P- wave  $B\bar{B}$  interaction is not so strong. From this observation, we may get an upper limit of the cutoff,  $\Lambda < 2.0$  GeV. In fact, investigation in detail reduces the upper limit to 1.7 GeV where there is a shallow P- wave resonance.

## VII. DISCUSSIONS

From the calculated partial wave phase shifts, we know that neither the  $D\bar{D}$  nor the  $B\bar{B}$  bound state exists if one does not consider the vector meson exchange interaction. One gets the same conclusion from solving the bound state problem. Furthermore, in this case, the interactions for the isoscalar and isovector systems are the same, and therefore are not reasonable. The realistic interactions in the meson exchange models should include the vector meson contributions, and then the isoscalar interaction becomes more attractive. Our following discussions concentrate on the case  $I = 0$  and VC.

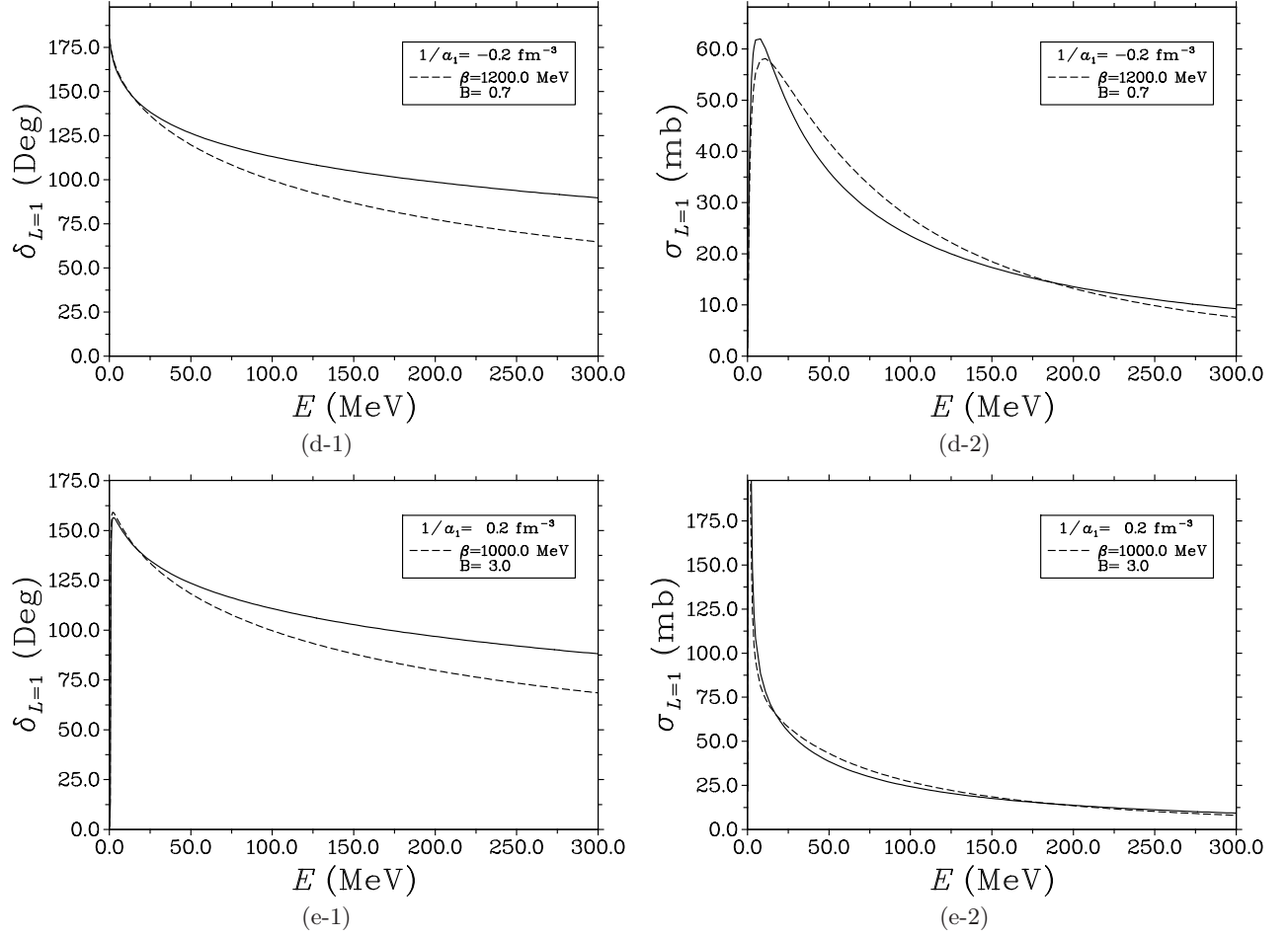


FIG. 12: The first (last) two diagrams show the reproduced P-wave  $B\bar{B}$  phase shifts and scattering cross sections corresponding to the case (d) [(e)] with  $1/a_1 = -0.18$  ( $0.22$ )  $\text{fm}^{-3}$ , respectively.

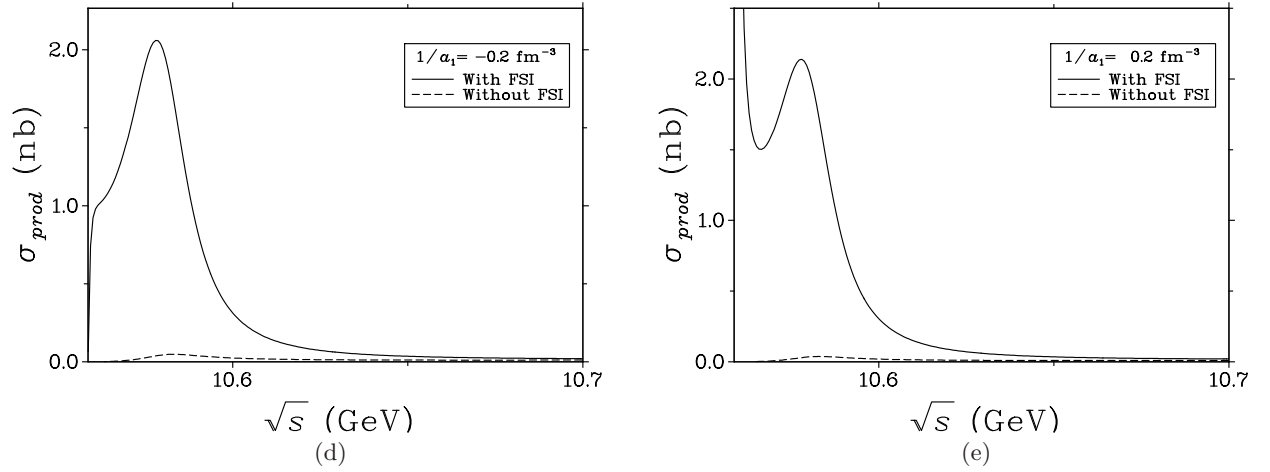


FIG. 13: The obtained  $B\bar{B}$  production cross sections correspond to the case (d)  $1/a_1 = -0.18 \text{ fm}^{-3}$  and (e)  $1/a_1 = 0.22 \text{ fm}^{-3}$ , respectively. We get the dashed lines by ignoring the rescattering part  $\sigma_2$  of the production cross section  $\sigma_{prod} = \sigma_1 + \sigma_2$ .



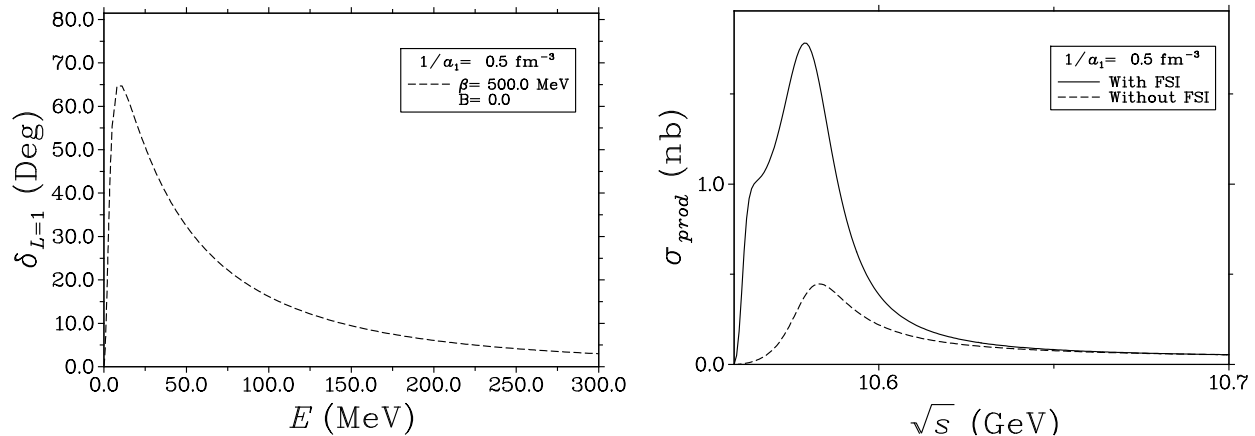


FIG. 14: The obtained  $B\bar{B}$  phase shifts and production cross sections for the case  $1/a_1=0.5 \text{ fm}^{-3}$ . We get the dash line in the right diagram by ignoring the rescattering part  $\sigma_2$  of the production cross section  $\sigma_{prod} = \sigma_1 + \sigma_2$ .

First, we focus on the cutoff  $\Lambda$  in our model study of  $D\bar{D}$  and  $B\bar{B}$ , which is to be almost universal for the bound state problem, the scattering problem, and the production problem. The sensitivity to the cutoff requires a reasonable range. This parameter for  $B\bar{B}$  should be a little larger than that for  $D\bar{D}$  and thus the upper limit from the former case applies to the latter case. Here we get an upper limit  $\Lambda < 1.7 \text{ MeV}$  from the  $B\bar{B}$  production cross section and the P- wave interaction. We may constrain the cutoff from the P- wave  $B\bar{B}$  process because the possible resonance or bound state in the rescattering mechanism changes the line shape of the cross section. Since neither a P- wave resonance nor a bound state exists, one cannot get the constraint from the  $D\bar{D}$  production.

With the upper limit 1.7 GeV of the cutoff, we cannot exclude the possible  $D\bar{D}$  S-wave bound state, but the binding energy is less than 10 MeV. There does not exist a P- wave  $B\bar{B}$  bound state or a resonance, while the binding energy of the possible S- wave molecule should be below 100 MeV. We have used the vector meson coupling constants  $g_V$  and  $\beta_V$  derived from the vector meson dominance. The recent calculation with light cone QCD sum rule method gives a smaller  $g_V \cdot \beta_V$  [48]. It will lead to shallower meson-meson bound states.

In our calculation, we have used a monopole type form factor in the meson exchange potential. One may alternatively choose a dipole type form factor. The potential in the latter case is weaker than that in the former one if the same cutoff is adopted. Provided one obtains the same scattering volume with  $\Lambda_1$  in the monopole case and  $\Lambda_2$  in the dipole case,  $\Lambda_2$  is larger than  $\Lambda_1$ . The corresponding S- wave binding energies have the relation  $|E_1| > |E_2|$ , but the difference is small. From the normal line shape of the  $B\bar{B}$  production cross section and the P- wave interaction, we find that the cutoff now should be smaller than 2.4 GeV. The corresponding binding energies for the possible S- wave molecules change a little, but we still have the results:  $E_{D\bar{D}} < 10 \text{ MeV}$  and  $E_{B\bar{B}} < 100 \text{ MeV}$ . That is, the usage of a different form factor has small effect on the constrain for the S- wave binding energies.

If the  $D\bar{D}$  S- wave bound state exists, its strong decay channel would be mainly  $\eta_c\eta$  and  $\chi_{c0}\pi\pi$ . Other channels such as  $\eta_c\pi\pi\pi$  and  $J/\psi\pi\pi\pi$  are suppressed. This state may be produced in  $B$  decay,  $\gamma\gamma$  fusion and  $p\bar{p}$  collision [49]. Future precision analysis of the process  $e^+e^- \rightarrow J/\psi + \text{scalar states}$  may also offer a chance to find it. On the other hand, since the  $B\bar{B}$  bound state is close to the thresholds of  $\Upsilon(1S)\phi$  and  $\chi_{b0}(2P)\pi\pi$ , its dominant strong decay channels would be  $\Upsilon(1S)\omega$  and  $\chi_{b0}(1P)\pi\pi$ . One has a chance to obtain this scalar state by  $p\bar{p}$  collision.

In our approach, the S- and P- wave  $D\bar{D}$  interactions depend on the same cutoff. Once the P- wave production including the final state interactions gives a constraint on its reasonable range, the S- wave interactions are better understood. This approach may be applied to new exotic resonances which are candidates of S- wave meson-antimeson molecules. For example, the P- wave  $D^*\bar{D}^*$  production will be helpful to understand  $Z^+(4051)$  [50] and the relevant bound state problem [51, 52]. The cutoff  $\Lambda$  will not change significantly because of the heavy quark symmetry. Another interesting example is the  $D\bar{D}^*$  interaction. The investigation on their P- wave production may deepen our knowledge about  $X(3872)$  [53, 54].

From the study of the P- wave  $B\bar{B}$  production by including the rescattering effects, we have seen the result in the separable approximation is sensitive to both the amplitude and the sign of the scattering volume  $a_1$ . If there is a shallow bound state or a sharp resonance, the line shape of the production cross section may reflect that structure, which is difficult to identify just from the scattering cross sections. The S- wave production processes should have a similar feature. Since the S- wave system has stronger attraction, that process is more interesting. Such a study is expected to be helpful to understand some of the newly observed near-threshold structures.

In summary, we have explored the bound state and the scattering problem for the isoscalar  $D\bar{D}$  system, and the

rescattering effects in the  $e^+e^- \rightarrow D\bar{D}$  process. We have also considered the corresponding bottom cases. From the binding energies and the phase shifts, the S- wave  $D\bar{D}$  bound state would exist if the vector meson exchange interaction plays a major role. From the line shape of the calculated  $D\bar{D}$  production cross section, it is difficult to understand the BES observation by the  $D\bar{D}$  rescattering effect. From the line shape of the  $B\bar{B}$  production cross section, we have estimated the upper limit of the cutoff  $\Lambda$  in the coupling form factor (monopole type) to be 1.7 GeV. Assuming this is the case, we get an upper limit of the S- wave binding energy: 10 MeV for  $D\bar{D}$  and 100 MeV for  $B\bar{B}$ . The future measurement of the S- and P- wave phase shifts, scattering length or volume, and the production cross sections may provide more information about the near-threshold resonances.

### Acknowledgments

We thank Professors Z.Y. Zhang, P.N. Shen, X.Y. Shen, and Q. Zhao for helpful discussions. This project was supported partly by the Japan Society for the Promotion of Science under Contract No. P09027; KAKENHI under Contract Nos. 17070002 (Priority area), 19540275, 20540281, 22105503, and 21-09027; National Natural Science Foundation of China under Grant Nos. 10625521, 10675008, 10705001, 10775146, 10721063, and 10805048; the Foundation for the Author of National Excellent Doctoral Dissertation of P.R. China (FANEDD) under Contract No. 200924; the Doctoral Program Foundation of Institutions of Higher Education of P.R. China under Grant No. 20090211120029; and the Program for New Century Excellent Talents in University (NCET) by the Ministry of Education of P.R. China under Grant No. NCET-10-0442.

### Appendix A: Production cross section

Here, we illustrate the procedure to derive the production cross section after considering the rescattering effects. We use the PDG state normalization  $\langle \vec{p} | \vec{q} \rangle = (2\pi)^3 \delta^3(\vec{p} - \vec{q})$  [46]. In the center of mass (c.m.) frame, the  $D\bar{D}$  system with the c.m. momentum  $\vec{p}$  also has this normalization. Therefore, one has

$$1 = \sum_f \int \frac{d^3 \vec{p}_f}{(2\pi)^3} |\vec{p}_f\rangle \langle \vec{p}_f|. \quad (\text{A1})$$

Our basic formula is the differential cross section for a  $2 \rightarrow 2$  production process [46]

$$d\sigma = \frac{|M|^2}{4F_f} (2\pi)^4 \delta^4(P - \sum p_f) \frac{d^3 \vec{p}_{f1} d^3 \vec{p}_{f2}}{(2\pi)^3 (2E_{f1}) (2\pi)^3 (2E_{f2})}, \quad (\text{A2})$$

where  $M$  is the Lorentz-invariant scattering amplitude,  $F_f$  is the flux factor and  $\vec{p}(E_f)$  is the 3-momentum (energy) of the final state meson.

To consider FSI, we insert Eq. (A1) into  $|M|^2$ :

$$\begin{aligned} |M|^2 &= |\langle f | \hat{O} | i \rangle|^2 = \left| \sum_m \int \frac{d^3 \vec{p}_m}{(2\pi)^3} \langle f | \hat{O}_2 | m \rangle \langle m | \hat{O}_1 | i \rangle \right|^2 \\ &= \sum_{m_1, m_2} \int \frac{d^3 \vec{p}_{m_1}}{(2\pi)^3} \int \frac{d^3 \vec{p}_{m_2}}{(2\pi)^3} \left[ \langle i | \hat{O}_1^\dagger | m_2 \rangle \langle m_1 | \hat{O}_1 | i \rangle \right] \left[ \langle m_2 | \hat{O}_2^\dagger | f \rangle \langle f | \hat{O}_2 | m_1 \rangle \right]. \end{aligned} \quad (\text{A3})$$

Here, the operator  $\hat{O}_1$  describes the production of  $D\bar{D}$  and  $\hat{O}_2$  describes the rescattering of the final states  $D\bar{D}$ .  $\vec{p}_{m_1}$  and  $\vec{p}_{m_2}$  are the momenta in the c.m. frame. They have different angles but the same amplitude. One may get the total cross section

$$\begin{aligned} \sigma &= \frac{1}{4F_f} \int \frac{d^3 \vec{p}_{m_1}}{(2\pi)^3} \int \frac{d^3 \vec{p}_{m_2}}{(2\pi)^3} \frac{1}{(2E_{m_1})(2E_{m_2})} \left[ \langle i | \hat{O}_1^\dagger | m_2 \rangle \langle m_1 | \hat{O}_1 | i \rangle \right] \int \frac{d^3 \vec{p}_f}{(2\pi)^3} \left[ \langle m_2 | \hat{O}_2^\dagger | f \rangle \langle f | \hat{O}_2 | m_1 \rangle \right] \\ &\quad \times (2\pi) \delta(E - 2E_f) \\ &= \frac{1}{2s} \int \frac{d^3 \vec{p}}{(2\pi)^3} \int \frac{d^3 \vec{q}}{(2\pi)^3} \frac{1}{(2E_p)(2E_q)} \left[ \langle i | \hat{O}_1^\dagger | \vec{q} \rangle \langle \vec{p} | \hat{O}_1 | i \rangle \right] S(E), \end{aligned} \quad (\text{A4})$$

where we have ignored the mass of the electron and have used  $F_f = s/2$ .

We calculate the first part as follows

$$\langle i|\hat{O}_1^\dagger|\vec{q}\rangle\langle\vec{p}|\hat{O}_1|i\rangle = \frac{8e^4}{s^2}[-4\vec{k}\cdot\vec{p}\vec{k}\cdot\vec{q} + \vec{p}\cdot\vec{q}s] \times |\text{f.f.}|^2, \quad (\text{A5})$$

where  $\vec{k}$  is the momentum of the initial electron in the c.m. frame and f.f. has been given in Eq. (9).

For the second part in Eq. (A4), we have

$$\begin{aligned} S(E) &\equiv \int \frac{d^3\vec{p}_f}{(2\pi)^3} \left[ \langle\vec{q}|\hat{O}_2^\dagger|f\rangle\langle f|\hat{O}_2|\vec{p}\rangle \right] (2\pi)\delta(E - 2E_f) \\ &= -2\text{Im} \left[ \langle\vec{q}|\hat{G}(E)|\vec{p}\rangle \right] \end{aligned} \quad (\text{A6})$$

with  $\hat{G}(E) = [E - \hat{H} + i\epsilon]^{-1}$ . When there is no FSI,  $\hat{G}(E) = \hat{G}^0(E) = [E - \hat{H}^0 + i\epsilon]^{-1}$ ,  $H^0 = 2(m_D + \frac{p^2}{2m_D}) \approx 2E_f$ . In general,

$$\begin{aligned} \hat{G}(E) &= \hat{G}^0(E) + \hat{G}^0(E)V_{int}\hat{G}^0(E) + \dots \\ &= \frac{1}{1 - \hat{G}^0(E)V_{int}}\hat{G}^0(E), \end{aligned} \quad (\text{A7})$$

where  $V_{int}$  is the potential.

To get the analytical expression of the cross section, we adopt the Yamaguchi separable approximation [35]. For the P-wave  $DD$  interaction, one may write down as

$$\langle\vec{p}|V_{int}|\vec{q}\rangle = -\frac{\lambda}{m_D}g(\vec{p})\cdot g(\vec{q}), \quad g(\vec{p}) = \beta t(p)\vec{p}. \quad (\text{A8})$$

We determine  $\lambda$ ,  $\beta$  and other parameters in the function  $t(p)$  through reproducing the calculated phase shifts and the scattering cross section. After some calculations, one finally gets

$$S(E) = (2\pi)^4\delta(E - E_p - E_q)\delta^3(\vec{p} - \vec{q}) + \frac{2\lambda}{m_D}\text{Im} \left[ \frac{\tilde{g}(\vec{p})\cdot\tilde{g}(\vec{q})}{1 + \frac{\lambda W}{3m_D}} \right]. \quad (\text{A9})$$

In this formula,

$$\tilde{g}(\vec{k}) = g(\vec{k})[E - 2m_D - \frac{k^2}{m_D} + i\epsilon]^{-1}, \quad (\text{A10})$$

$$W \equiv \int \frac{d^3\vec{k}}{(2\pi)^3} \frac{g(\vec{k})\cdot g(\vec{k})}{E - 2m_D - k^2/m_D + i\epsilon}. \quad (\text{A11})$$

With the equation  $\frac{1}{E-H+i\epsilon} = \frac{\mathcal{P}}{E-H} - i\pi\delta(E-H)$ , it is easy to get the real part and the imaginary part

$$\text{Re}W = -m_D\frac{\beta^2}{2\pi^2}\mathcal{P}\int_0^\infty dk \frac{k^4}{k^2 - \alpha^2} [t(k)]^2, \quad (\text{A12})$$

$$\text{Im}W = -m_D\frac{\beta^2\alpha^3}{4\pi} [t(\alpha)]^2, \quad (\text{A13})$$

where  $\alpha^2 \equiv m_D(E - 2m_D)$ .

By combining Eqs. (A4), (A5), and (A9), we obtain the resultant cross section  $\sigma = \sigma_1 + \sigma_2$ ,

$$\sigma_1 = \frac{\pi}{3}\alpha_e^2 \frac{(s - 4m_D^2)^{3/2}}{s^{5/2}} \times |\text{f.f.}|^2, \quad (\text{A14})$$

$$\sigma_2 = \frac{64}{9} \frac{\pi^2\alpha_e^2\lambda}{s^2m_D} \text{Im} \left\{ \left(1 + \frac{\lambda W}{3m_D}\right)^{-1} U^2 \right\} \times |\text{f.f.}|^2, \quad (\text{A15})$$

where  $\alpha_e = 1/137$  and

$$U \equiv \beta \int \frac{d^3\vec{p}}{(2\pi)^3} \frac{p^2}{(2E_p)} \frac{t(p)}{E - 2m_D - \frac{p^2}{m_D} + i\epsilon}$$

$$\simeq 4\pi m_D \beta \int_0^\infty \frac{dp}{(2\pi)^3} \frac{p^4}{p^2 + 2m_D^2} \frac{t(p)}{E - 2m_D - \frac{p^2}{m_D} + i\epsilon}, \quad (\text{A16})$$

$$\text{Re}U = -m_D^2 \frac{\beta}{2\pi^2} \mathcal{P} \int_0^\infty dk \frac{k^4}{(k^2 + 2M^2)(k^2 - \alpha^2)} t(k), \quad (\text{A17})$$

$$\text{Im}U \approx -m_D \frac{\beta \alpha^3}{4\pi\sqrt{s}} t(\alpha). \quad (\text{A18})$$

If one defines  $W^r = 1 + \frac{\lambda}{3m_D} \text{Re}W$ ,  $W^i = \frac{\lambda}{3m_D} \text{Im}W$ , then

$$\sigma_2 = \frac{64 \pi^2 \alpha_e^2 \lambda}{9 s^2 m_D} \left\{ \frac{2(\text{Re}U \times \text{Im}U)W^r - [(\text{Re}U)^2 - (\text{Im}U)^2]W^i}{(W^r)^2 + (W^i)^2} \right\} \times |\text{f.f.}|^2. \quad (\text{A19})$$

When there is no FSI,  $\lambda = 0$  and  $\sigma_2$  vanishes.

### Appendix B: The parameters

Before the numerical evaluation, we have to choose the form of the function  $t(k)$  and determine the relevant parameters. In Ref. [55], the separable P- wave potential was given with  $t(k) = \frac{1}{(k^2 + \beta^2)^2}$ . However, we find the following choice is better when reproducing the scattering cross sections:

$$t(k) = \frac{1}{(k^2 + \beta^2)^2} + \frac{B}{\beta^2(k^2 + \beta^2)}, \quad (\text{B1})$$

where  $B$  is a dimensionless parameter. One notes the second term of  $g(\vec{k})$  does not have a good behavior at large  $k$ . This is easy to see after the Fourier transformation. Since we consider only low-energy interactions, this form is acceptable.

From the scattering amplitude, one has

$$k^3 \cot(\delta_1) = \frac{12\pi}{\lambda\beta^2[t(k)]^2} + \frac{4\pi F(k)}{\beta^2[t(k)]^2}, \quad (\text{B2})$$

$$F(k) = \frac{\beta^2}{2\pi^2} \mathcal{P} \int_0^\infty dq \frac{q^4}{k^2 - q^2} [t(q)]^2, \quad (\text{B3})$$

where  $\delta_1$  is the P- wave phase shift. According to the definition of the scattering volume  $a_1$ ,

$$\frac{1}{a_1} = \frac{4\pi}{\beta^2} \frac{F(0)}{[t(0)]^2} + \frac{12\pi}{\lambda\beta^2[t(0)]^2}. \quad (\text{B4})$$

So the coupling constant is

$$\lambda = \frac{12\pi}{\frac{1}{a_1} \beta^2 [t(0)]^2 - (4\pi)F(0)}. \quad (\text{B5})$$

If one does not explicitly use the coupling constant in expressing the P- wave cross section, we have

$$k^3 \cot(\delta_1) = \frac{4\pi[F(k) - F(0)]}{\beta^2[t(k)]^2} + \frac{1}{a_1} \frac{[t(0)]^2}{[t(k)]^2}, \quad (\text{B6})$$

$$\sigma_{L=1} = \frac{12\pi k^4}{k^6 + [k^3 \cot(\delta_1)]^2}. \quad (\text{B7})$$

By inserting the function  $t(k)$  into the above formulas, it is easy to get the explicit expressions which we do not present here. The scattering volume has been derived in Sec IV. Now the parameters we have to determine are  $\beta$  and  $B$ . They are extracted by reproducing the  $\delta_1$  and  $\sigma_{L=1}$ .

- 
- [1] E.S. Swanson, Phys. Rep. **429**, 243 (2006).  
[2] M.B. Voloshin, Prog. Part. Nucl. Phys. **61**, 455 (2008); arXiv: 0711.4556 [hep-ph].  
[3] S. Godfrey and S.L. Olsen, Ann. Rev. Nucl. Part. Sci. **58**, 51 (2008); arXiv: 0801.3867 [hep-ph].  
[4] S.L. Zhu, Int. J. Mod. Phys. E **17**, 283 (2008); arXiv: 0707.2623 [hep-ph].  
[5] S.L. Olsen, arXiv: 0909.2713 [hep-ex]; C.Z. Yuan, arXiv: 0910.3138 [hep-ex]; A. Zupanc, arXiv: 0910.3404 [hep-ex]; S. Godfrey, arXiv: 0910.3409 [hep-ph].  
[6] B.Q. Li and K.T. Chao, Phys. Rev. D **79**, 094004 (2009); B.Q. Li, C. Meng, and K.T. Chao, Phys. Rev. D **80**, 014012 (2009).  
[7] X. Liu, Z. G. Luo and Z. F. Sun, Phys. Rev. Lett. **104**, 122001 (2010) [arXiv:0911.3694 [hep-ph]].  
[8] N.A. Törnqvist, Z.Phys. C **61**, 525 (1994).  
[9] Y.J. Zhang, H.C. Chiang, P.N. Shen, and B.S. Zou, Phys. Rev. D **74**, 014013 (2006).  
[10] Y.R. Liu, X. Liu, W.Z. Deng and S.L. Zhu, Eur. Phys. J. C **56**, 63 (2008).  
[11] X. Liu, Y.R. Liu, W.Z. Deng and S.L. Zhu, Phys. Rev. D **77**, 094015 (2008).  
[12] X. Liu, Y.R. Liu, W.Z. Deng and S.L. Zhu, Phys. Rev. D **77**, 034003 (2008) [arXiv:0711.0494 [hep-ph]].  
[13] Y.R. Liu, Z.Y. Zhang, Phys. Rev. C **79**, 035206 (2009).  
[14] X. Liu, Z.G. Luo, Y.R. Liu, S.L. Zhu, Eur. Phys. J. C **61**, 411 (2009).  
[15] X. Liu and S.L. Zhu, Phys. Rev. D **80**, 017502 (2009) [arXiv:0903.2529 [hep-ph]].  
[16] Y.R. Liu and Z.Y. Zhang, Phys. Rev. C **80**, 015208 (2009).  
[17] G.J. Ding, J.F. Liu, and M.L. Yan, Phys. Rev. D **79**, 054005 (2009).  
[18] C.Y. Wong, Phys. Rev. C **69**, 055202 (2004).  
[19] G.J. Ding, W. Huang, J.F. Liu, and M.L. Yan, Phys. Rev. D **79**, 034026 (2009).  
[20] D. Gamermann, E. Oset, D. Strottman, and M.J. Vicente Vacas, Phys. Rev. D **76**, 074016 (2007)  
[21] T.W. Chiu and T.H. Hsieh, Phys. Rev. D **73**, 094510 (2006); Phys. Lett. B **646**, 95 (2007).  
[22] S.H. Lee, M. Nielsen, U. Wiedner, arXiv: 0803.1168 [hep-ph]; R.M. Albuquerque, M. Nielsen, Nucl. Phys. A **815**, 53 (2009); J.R. Zhang and M.Q. Huang, Phys. Rev. D **80**, 056004 (2009).  
[23] D. Gamermann, E. Oset, Eur. Phys. J. A **36**, 189 (2008).  
[24] M.L. de Farias Freire, R.R. da Silva, arXiv: 1003.1690 [hep-ph].  
[25] D. Zhang, Q.Y. Zhao, Q.Y. Zhang, Chin. Phys. Lett. **26**, 091201 (2009).  
[26] D.L. Canham, H.W. Hammer, R.P. Springer, Phys. Rev. D **80**, 014009 (2009).  
[27] M. Ablikim et al. (BES Collaboration), Phys. Rev. Lett. **101**, 102004 (2008); 0807.0494.  
[28] M. Ablikim et al. (BES Collaboration), Phys. Lett. B **668**, 263 (2008).  
[29] S. Dubynskiy, M.B. Voloshin, Phys. Rev. D **78**, 116014 (2008).  
[30] X. Liu, B. Zhang, X.Q. Li, Phys. Lett. B **675**, 441 (2009).  
[31] Y.J. Zhang, G. Li, and Q. Zhao, Phys. Rev. Lett. **102**, 172001 (2009).  
[32] M. Ablikim et al., BES Collaboration, Phys. Rev. D **76**, 122002 (2007).  
[33] M. Ablikim et al., BES Collaboration, Phys. Lett. B **659**, 74 (2008).  
[34] Y.J. Zhang, and Q. Zhao, Phys. Rev. D **81**, 034011 (2010).  
[35] Y. Yamaguchi, Phys. Rev. **95**, 1628 (1954).  
[36] R. Casalbuoni, A. Deandrea, N. Di Bartolomeo, R. Gatto, F. Feruglio and G. Nardulli, Phys. Rep. **281**, 145 (1997).  
[37] W.A. Bardeen, E.J. Eichten, C.T. Hill, Phys. Rev. D **68**, 054024 (2003).  
[38] C. Isola, M. Ladisa, G. Nardulli, P. Santorelli, Phys. Rev. D **68**, 114001 (2003).  
[39] E. Fermi and C.N. Yang, Phys. Rev. **76**, 1739 (1949).  
[40] S. Ishida et al., Prog. Theor. Phys. **95**, 745 (1996).  
[41] K. Igi, K.I. Hikasa, Phys. Rev. D **59**, 034005 (1999).  
[42] G. Colangelo, J. Gasser, H. Leutwyler, Nucl. Phys. B **603**, 125 (2001); I. Caprini, G. Colangelo, H. Leutwyler, Phys. Rev. Lett. **96**, 132001 (2006).  
[43] M.Z. Yang, Mod. Phys. Lett. A **23**, 3113 (2008).  
[44] H.B. Li, X.S. Qin, M.Z. Yang, Phys. Rev. D **81**, 011501(R) (2010).  
[45] M. Takizawa and S. Takeuchi, EPJ web of conference **3**, 03026 (2010).  
[46] C. Amsler et al. (Particle Data Group), Phys. Lett. B **667**, 1 (2008).  
[47] B. Aubert et al. (BaBar Collaboration), Phys. Rev. Lett. **102**, 012001 (2009).  
[48] P.Z. Huang, L. Zhang, and S.L. Zhu, Phys. Rev. D **80**, 014023 (2009).  
[49] M. Andreotti et al. (Fermilab E835 Collaboration), Phys. Rev. Lett. **91**, 091801 (2003).  
[50] R. Mizuk et al. (Belle Collaboration), Phys. Rev. D **78**, 072004 (2008).  
[51] A.D. Rujula, H. Georgi and S.L. Glashow, Phys. Rev. Lett. **38**, 317 (1977).  
[52] S. Dubynskiy and M.B. Voloshin, Mod. Phys. Lett. A **21**, 2779 (2006).

- [53] G. Pakhlova et. al. (Belle Collaboration), Phys. Rev. Lett. **98**, 092001 (2007).
- [54] B. Aubert et. al. (BaBar Collaboration), Phys. Rev. D **79**, 092001 (2009).
- [55] Y. Nogami, W. van Dijk, Phys. Rev. C **34**, 1855 (1986).